การดัดแปรผิวควอนตัมดอตของซิงก์ซีลีไนด์/ซิงก์ซัลไฟด์ด้วยพอลิเมอร์ที่เข้ากันได้ทางชีวภาพสำหรับการประยุกต์ทางชีวภาพ

นางสาวรดาวรรณ ปาลิกานนท์

วิทยานิพนธ์นี้เป็นส่วนหนึ่งของการศึกษาตามหลักสูตรปริญญาวิทยาศาสตรมหาบัณฑิต
สาขาวิชาปิโตรเคมีและวิทยาศาสตร์พอลิเมอร์
คณะวิทยาศาสตร์ จุฬาลงกรณ์มหาวิทยาลัย
ปีการศึกษา 2559

SURFACE MODIFICATION OF ZnSe/ZnS QUANTUM DOTS WITH BIOCOMPATIBLE POLYMER FOR BIOLOGICAL APPLICATIONS

Miss Radawan Palikanon

A Thesis Submitted in Partial Fulfillment of the Requirements
for the Degree of Master of Science Program in Petrochemistry and Polymer Science
Faculty of Science
Chulalongkorn University
Academic Year 2016

Thesis Title	SURFACE MODIFICATION OF ZnSe/ZnS QUANTUM DOTS WITH BIOCOMPATIBLE POLYMER FOR BIOLOGICAL APPLICATIONS
By	Miss Radawan Palikanon
Field of Study	Petrochemistry and Polymer Science
Thesis Advisor	Numpon Insin, Ph.D.

Accepted by the Faculty of Science, Chulalongkorn University in Partial Fulfillment of the Requirements for the Master's Degree

.....Dean of the Faculty of Science

(Associate Professor Polkit Sangvanich, Ph.D.)

THESIS COMMITTEE

.....Chairman

(Assistant Professor Warinthorn Chavasiri, Ph.D.)

.....Thesis Advisor

(Numpon Insin, Ph.D.)

.....Examiner

(Varagorn Hengpunya, Ph.D.)

.....External Examiner

(Assistant Professor Chuda Chittasupho, Ph.D.)

รดาวรรณ ปาลิกานนท์ : การดัดแปรผิวควอนตัมดอตของซิงก์ซีลีไนด์/ซิงก์ซัลไฟด์ด้วยพอลิเมอร์ที่เข้ากันได้ทางชีวภาพสำหรับการประยุกต์ทางชีวภาพ (SURFACE MODIFICATION OF ZnSe/ZnS QUANTUM DOTS WITH BIOCOMPATIBLE POLYMER FOR BIOLOGICAL APPLICATIONS) อ.ที่ปรึกษาวิทยานิพนธ์หลัก: ดร.นำพล อินสิน, 64 หน้า.

ในงานวิจัยนี้ได้สังเคราะห์และดัดแปรอนุภาคควอนตัมดอตระดับนาโนชนิดซิงค์ซีลีไนด์/ซิงค์ (ZnSe/ZnS QDs) เพื่อนำไปประยุกต์ทางชีวภาพ โดยได้สังเคราะห์อนุภาคควอนตัมดอตซิงค์ซีลีไนด์/ซิงค์ซัลไฟด์โดยใช้ซิงค์สเตียเรตเป็นสารตั้งต้นและ1-octadecene เป็นตัวทำละลายโดยใช้วิธีการฉีดที่อุณหภูมิสูงในขั้นตอนเดียว ซิงค์ซีลีไนด์/ซิงค์ซัลไฟด์ควอนตัมดอตที่ได้ถูกนำไปพิสูจน์เอกลักษณ์โดยใช้เครื่องยูวี-วิสิเบิล สเปคโตรสโคปี, ฟลูออเรสเซนต์ สเปคโตรสโคปีและเทคนิคการส่องภาพจากกล้องจุลทรรศน์อิเล็กตรอนแบบส่องผ่านซึ่งผลที่ได้พบว่า อนุภาคควอนตัมดอตซิงค์ซีลีไนด์/ซิงค์ซัลไฟด์ปล่อยการเรืองแสงสีน้ำเงินออกมาที่ความยาวคลื่นประมาณ 400-450 นาโนเมตรและ มีความกว้างของสัญญาณที่กึ่งกลางของสัญญาณสูงสุดที่แคบประมาณ 20-30 นาโนเมตร สำหรับผลของภาพจากกล้องจุลทรรศน์อิเล็กตรอนแบบส่องผ่านสามารถบอกขนาดและโครงสร้างของอนุภาคควอนตัมดอตซิงค์ซีลีไนด์/ซิงค์ซัลไฟด์โดยพบว่าอนุภาคมีเส้นผ่านศูนย์กลางเฉลี่ย 3.8 ± 0.4 นาโนเมตร โดยขนาดของอนุภาคเพิ่มขึ้นเมื่อเทียบกับอนุภาคก่อนเคลือบ ด้วยเปลือกหุ้มซิงค์ซัลไฟด์ นอกจากนี้ เพื่อปรับปรุงความสามารถในการกระจายตัวของอนุภาคสารละลายน้ำและลดความเป็นพิษของอนุภาคควอนตัมดอตลง งานวิจัยนี้ได้ดัดแปรอนุภาคควอนตัมดอตซิงค์ซีลีไนด์/ซิงค์ซัลไฟด์ด้วยลิแกนด์ที่มีหมู่ไทออลต่อกับพอลิอะมิโดเอมีน (PAMAM) โดยใช้วิธีแลกเปลี่ยนลิแกนด์ ผลการทดลองพบว่า ZnSe/ZnS quantum dots 4-(3,5-bis(mercaptomethyl)phenoxy) butanoic acid poly(amidoamine) (ZnSe/ZnS QDs-BMPBA-PAMAM) มีประสิทธิภาพที่ดีและมีการเชื่อมต่อที่แข็งแรงมากกว่า ZnSe/ZnS quantum dots dihydrolipoic acid poly(amidoamine) (ZnSe/ZnS QDs-DHLA-PAMAM) สำหรับการศึกษาความเป็นพิษต่อเซลล์โดยการวิเคราะห์ methylthiazolyldiphenyltetrazolium bromide (MTT) โดยเปรียบเทียบ ซิงค์ซีลีไนด์/ซิงค์ซัลไฟด์ควอนตัมดอต กับ แคดเมียมซีลีไนด์/ซิงค์ซัลไฟด์ควอนตัมดอต ที่ใช้กันอย่างแพร่หลาย จากผลการทดลองพบว่าอนุภาคควอนตัมดอตที่ใช้ซิงค์เป็นองค์ประกอบหลักมีความเป็นพิษต่ำกว่าอนุภาคควอนตัมดอตที่ใช้แคดเมียมเป็นองค์ประกอบหลัก และควอนตัมดอตที่ดัดแปรด้วยลิแกนด์ไทออลที่เชื่อมต่อด้วยพอลิเมอร์พอลิอะมิโดเอมีนมีความเข้ากันได้กับสิ่งมีชีวิตมากขึ้นเมื่อเปรียบเทียบกับควอนตัมดอตที่ไม่มีพอลิอะมิโดเอมีนเชื่อมต่อในลิแกนด์และเหมาะสมต่อการนำไปใช้งานทางด้านชีววิทยาต่อไป

สาขาวิชา ปิโตรเคมีและวิทยาศาสตร์พอลิเมอร์ ลายมือชื่อนิสิต .....

ปีการศึกษา 2559 ลายมือชื่อ อ.ที่ปรึกษาหลัก .....

5672060423 : MAJOR PETROCHEMISTRY AND POLYMER SCIENCE
KEYWORDS: QUANTUM DOTS / ZINC SELENIDE/ZINC SULFIDE / POLY(AMIDOAMINE) / PAMAM / LIGAND EXCHANGE

RADAWAN PALIKANON: SURFACE MODIFICATION OF ZnSe/ZnS QUANTUM DOTS WITH BIOCOMPATIBLE POLYMER FOR BIOLOGICAL APPLICATIONS. ADVISOR: NUMPON INSIN, Ph.D., 64 pp.

In this work, ZnSe/ZnS quantum dot nanoparticles (ZnSe/ZnS QDs) were synthesized and modified in order to apply in bio-application. ZnSe/ZnS QDs were synthesized using zinc stearate as zinc precursor and 1-octadecene as solvent by a hot-injection method in one-pot. The ZnSe/ZnS QDs were characterized using UV-visible spectroscopy, fluorescence spectroscopy and TEM. The photoluminescence of ZnSe/ZnS QDs was blue with the emission wavelength of about 400-450 nm and narrow full width at half maximum (FWHM) of about 20-30 nm. For TEM images, the results showed size and structure of ZnSe/ZnS QD nanoparticles. The average diameter of ZnSe/ZnS QDs particles was 3.8±0.4 nm. The size of ZnSe core QDs was increased upon coating with ZnS shell. In order to improve dispersibility in aqueous phase and reduce toxicity, ZnSe/ZnS QDs were modified with thiol-conjugated polyamidoamine (PAMAM) polymer by ligand exchange method. The results showed that ZnSe/ZnS QDs 4-(3,5-bis(mercaptomethyl)phenoxy)butanoic acid poly(amidoamine) (ZnSe/ZnS QDs-BMPBA-PAMAM) were obtained with higher efficiency than ZnSe/ZnS quantum dots dihydrolipoic acid poly(amidoamine) (ZnSe/ZnS QDs-DHLA-PAMAM). For cytotoxicity studied by methylthiazolyldiphenyltetrazolium bromide (MTT) assay, ZnSe/ZnS QDs were studied in comparison with the conventional CdSe/ZnS core-shell QDs. The Zn-based QDs exhibited lower toxicity than the Cd-based QDs, and the QDs that have been modified with thiol-conjugated PAMAM polymer showed higher biocompatibility than the ones without PAMAM and be more suitable for applying in biological applications.

Field of Study: Petrochemistry and Polymer Science Student's Signature .....
Advisor's Signature .....

Academic Year: 2016

ACKNOWLEDGEMENTS

Firstly, I would like to express the sense of gratitude and deeply appreciate Dr. Numpon Insin who is my thesis advisor, gave me valuable guidance and assistance to achieve in my thesis completely successful.

For valuable comment and advices, I would like to thank my thesis committee, Assistant Professor Dr. Warinthorn Chavasiri, the chairman, Dr. Numpon Insin, Dr. Varagorn Hengpunya and Assistant Professor Dr. Chuda Chittasupho. This research would have not been completed without all of their kindness.

Moreover, I would special thank Professor Dr. T. Randall Lee, University of Houston for kindness and generosity about BMPBA preparation. Also I would like to give thanks for Assist. Prof. Patcharee Ritprajak, Oral Biology Research Center, Faculty of Dentistry, Chulalongkorn University for the supporting about cytotoxicity studies and laboratory facilities and instruments.

In addition, I would like to thank all of members of Materials Chemistry and Catalyst Research Unit who are always helpful. Especially, Mr. Sarawuth Phaenthong, Miss Chalatan Saengruengrit, Miss Wishulada Injumpa Mr. Phranot Ajkidkarn, Miss Padtaraporn Chunhom, together with Mr. Rachata Weerapan and Mr. Panuwat Asavapannimit.

Finally, this work was supported by the CU Graduate School Thesis Grant (2016), Chulalongkorn University and partly supported by the Thailand Research Fund (TRF-RSA5780055); furthermore, I would like to greatly thank Petrochemistry and Polymer Science, Faculty of Science, Chulalongkorn University for the valuable instruments and laboratories. And I would like to thank family and friends for their helping, assistance and encouragement.

CONTENTS

Page

Page

LIST OF FIGURES

LIST OF TABLES

LIST OF ABBREVIATIONS

QDs	=	Quantum dots
ZnSe/ZnS QDs	=	Zinc selenide/ Zinc sulfide quantum dots
TA	=	Thiotic acid
DHLA	=	Dihydrolipoic acid
BMPBA	=	4-(3,5-bis(mercaptomethyl)phenoxy) butanoic acid
PAMAM	=	Poly(amidoamine)
ZnSe/ZnS QDs-DHLA-PAMAM	=	ZnSe/ZnS quantum dots dihydrolipoic acid poly(amidoamine)
ZnSe/ZnS QDs-BMPBA-PAMAM	=	ZnSe/ZnS quantum dots 4-(3,5-bis(mercaptomethyl)phenoxy)butanoic acid poly(amidoamine)
FWHM	=	Full width at half maximum
ZB	=	Zinc blende
WZ	=	Wurtzite
MTT assay	=	methylthiazolyldiphenyltetrazolium bromide assay
mL	=	Milliliter
μL	=	Microliter
h	=	Hour
min	=	Minute
g	=	Gram
mg	=	Milligram

CHAPTER I

INTRODUCTION

1.1 Statement of the problem

In recent years, nanomaterials have been used widely in biological applications. One of the novel nanomaterials is quantum dot. Quantum dots (QDs) are semiconductor nanomaterials that have a particle size of around 2-10 nm. The featured properties of quantum dots are their unique optical properties such as narrow emission, various fluorescence colors, visible with naked eye and photoluminescence stability. The fluorescent properties of QDs depend on their compositions and sizes. Quantum dots have been used in various applications such as bioimaging, biolabeling, biosensors, light-emitting diode (LED) and drug delivery. Generally, QDs are composed of three parts: core, shell and surface coating. The widely used QD cores are heavy metal cadmium-based QDs such as CdSe, CdS, and CdTe QDs. Although these QDs have many advantages and can be applied to many applications, they still have been concerned about toxicity when used. Moreover, the heavy metals in QDs have some risk to release into the natural environment leading to environmental impacts. Therefore, in this work, we aim at preparing QDs of different compositions by replacing the heavy metal cadmium-based QDs with zinc-based QDs in order to reduce toxicity problems.

Furthermore, other problems for using QDs in bio-applications are non-dispersibility in water phase and non-biocompatibility. Because the original synthesized QDs are coated with a hydrophobic stabilizing ligands for example trioctylphosphine (TOP) or trioctylphosphine oxide (TOPO), which were used to control the sizes of QDs during the synthesis, so it allows the QDs to be dispersed only in organic solvents. In order to improve solubility and transfer QDs into aqueous phase, QDs need to have hydrophilic ligands on their surface. Therefore, we are interested in ligand exchange method, which is one of the most used methods. In this method, new ligands can strongly bind onto particles, and the ligand can assist in particle stability with easy manipulation. Moreover, we also coat QDs with polymer

coating for increasing water dispersibility. Poly(amidoamine) or PAMAM dendrimers are one of promising polymers as they contain multiple functional groups for further conjugation and have been used in many biological applications. Moreover, PAMAM dendrimers are water soluble and biocompatible. In this thesis, we propose to synthesize the zinc-based QDs and improve their dispersibility in aqueous phase by coating with poly(amidoamine) polymer conjugated with thiol ligands using ligand exchange method with an aim at applying for bio-application.

1.2 Objectives

1. To synthesize Zn-based QD nanoparticles for replacing Cd-based QDs and obtaining QDs with lower toxicity
2. To modify ZnSe/ZnS QD nanoparticles with coating polymer for applying in biological systems.

1.3 Scope of this thesis

In this work, we have three main parts. First, we synthesized and prepared ZnSe/ZnS QDs. Second, we modified surface of ZnSe/ZnS QD nanoparticles using ligand exchange method by replacing the original ligands on the nanoparticle surface with the new ligands. The new ligands are hydrophilic ligand that could improve dispersibility of nanoparticles in aqueous media in order to use in biological applications. The ligands were synthesized and then conjugated with PAMAM polymer, and applied onto QD surface using ligand exchange method. Finally, the modified QDs conjugated with PAMAM polymer are investigated for cytotoxicity *in vitro* in comparison with Cd-based QDs by MTT assay.

1.4 The expected benefits

The benefits of this thesis are expected that the resulted ZnSe/ZnS QDs can be used in wide application similar to CdSe/ZnS QDs. Moreover, the ZnSe/ZnS QDs and the modified ZnSe/ZnS QDs should have low toxicity when compared with CdSe/ZnS QDs and become suitable for applying in biological applications in the future.

CHAPTER II

THOERY

2.1 Nanomaterials

The science of nanotechnology has been developed for many decades. Nanotechnology of nanomaterials or nanoparticles is a field about small scale materials that have particle size diameter between 1 nm to 100 nm. The nanomaterials are used in various applications; for examples, they are used for engineering electronic device and in biomedical application such as bioimaging, drug delivery and gene therapy. Nanoparticles have many benefits because they have high surface area and special property. Classification of nanomaterials composes of zero dimensional (0-D), one dimensional (1-D), two dimensional (2-D) and three dimensional (3-D) nanomaterials. The zero dimensional (0-D) have most tiny dimension within nanoscale in all directions. The most common representation of zero dimensional nanomaterials is nanoparticles or nanosphere such as semiconductor quantum dots (QDs). One dimensional (1-D) material has a long shape for examples nanotube, nanorod and nanowire. Next, the shape of two dimensional (2-D) nanoparticles is plane or sheet such as thin film. For the last type, three dimensional (3-D) nanomaterials is bulk materials that have higher surface area and adsorption sites such as nanoballs (dendritic structures), nanopillers, nanocones and nanoflowers. (**Figure 2.1**)

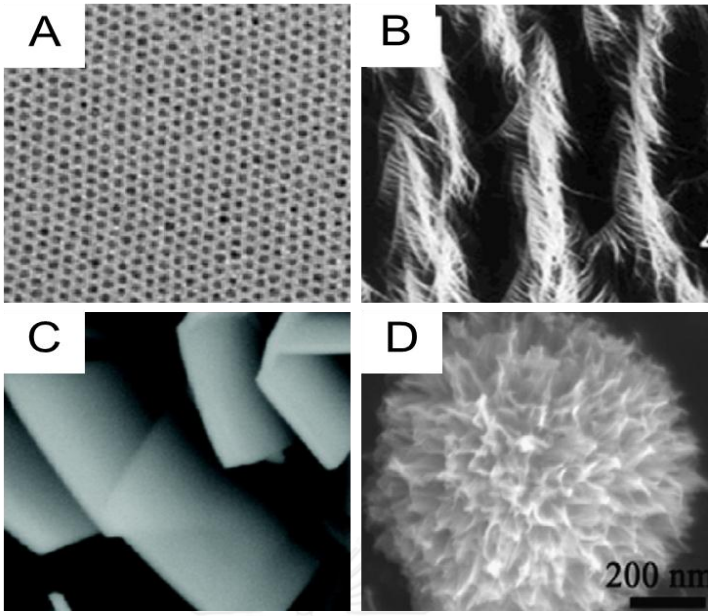

Figure 2.1 The examples of TEM and SEM images for each class of nanomaterials; (A) quantum dots nanoparticle (0-D), (B) nanofeather (1-D), (C) nanoplatelets (2-D) and (D) nanoflower (3-D) [1, 2]

2.2 Semiconductor quantum dots

Semiconductor quantum dots (QDs) are inorganic semiconductor nanocrystals that have a diameters ranging from 2 to 10 nm. QDs have unique optical, electronic and photoluminescence properties such as narrow emission, tunable luminescence and photostability [3]. The QDs are used in various applications [4, 5] as shown in **Figure 2.2.**

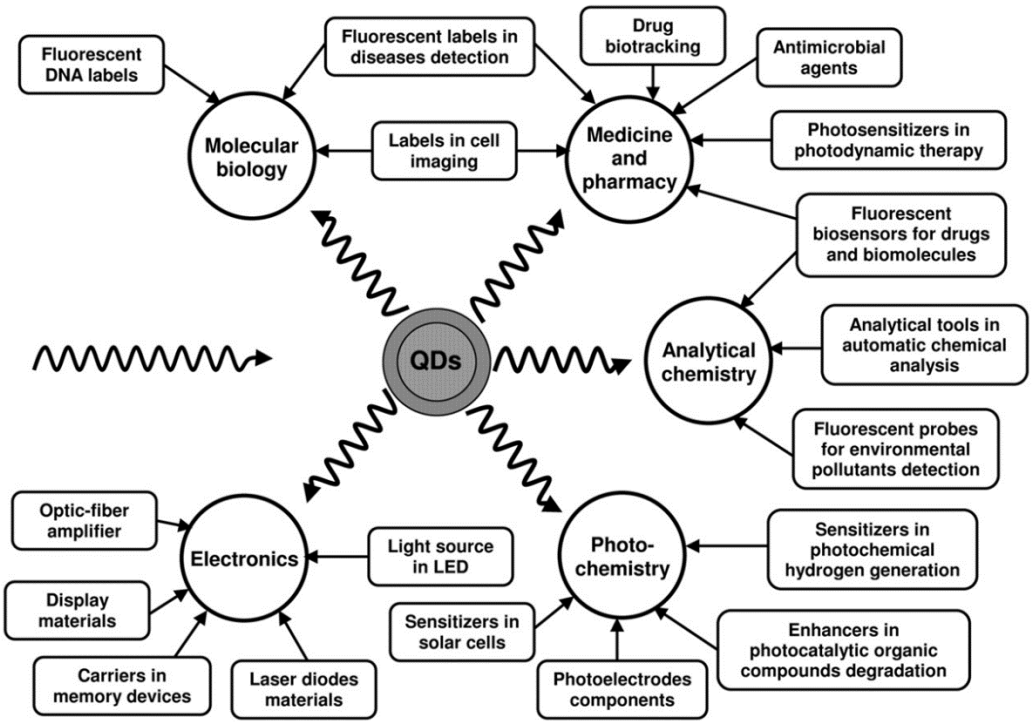

Figure 2.2 The versatile applications of QDs in various branches of science [6]

The fluorescence property of QDs arises from an electron in the electron–hole pairs movement between valence band and conduction band. When an electron is excited by UV radiation, it will move up from valence band to conduction band. The excited unstable electron relaxes by releasing energy in the term of fluorescence. Then relaxed electron back and fill in hole in valence band as shown in **Figure 2.3B**. The energy band gap between the valence band and the conduction depends on the size of QDs. The decrease in the size of quantum dot nanoparticles leads to enlargement of the energy band gap (higher energy), and the emission peak is in blue shift wavelength [7] as shown in **Figure 2.3 A**.

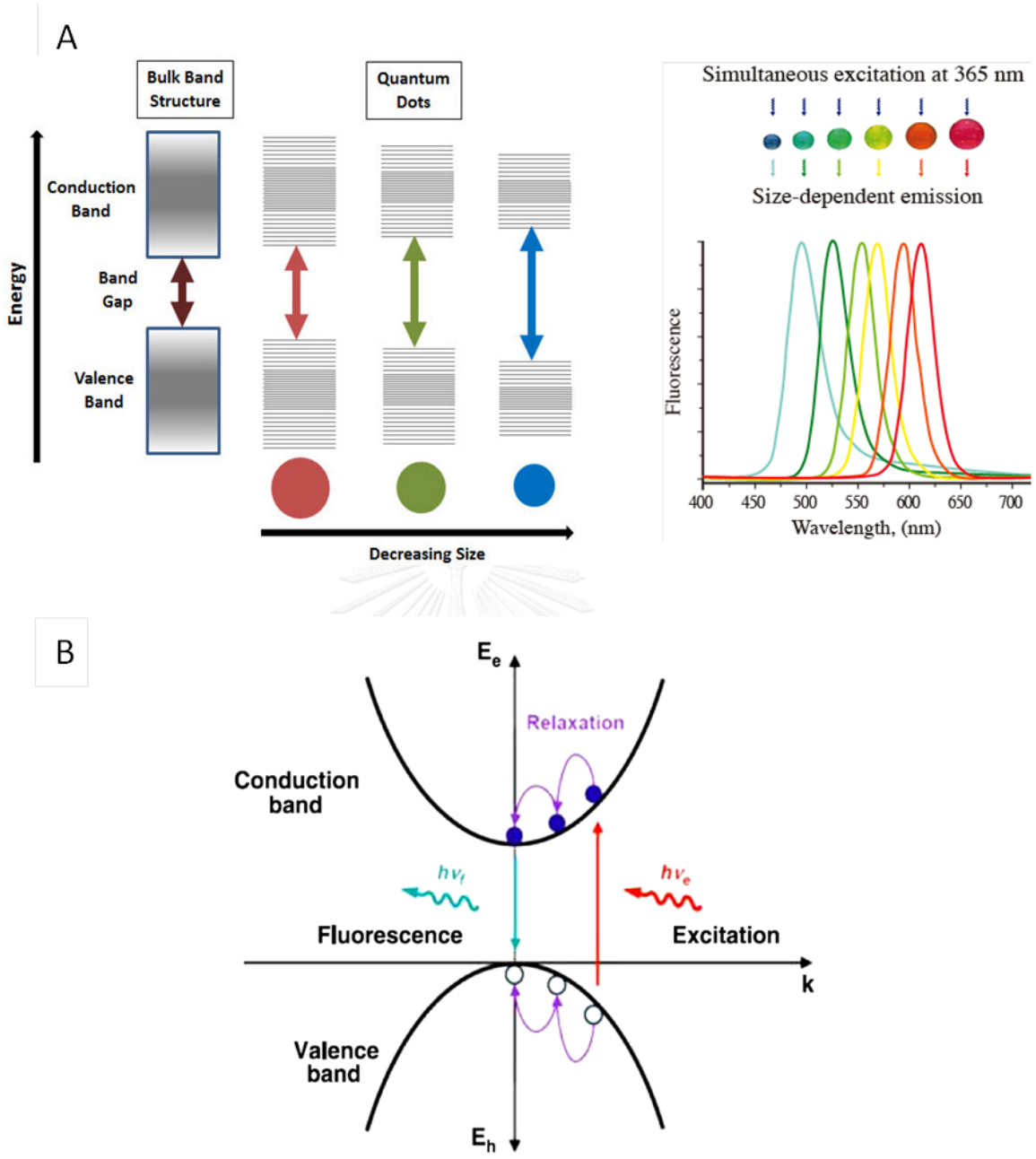

Figure 2.3 **(**A) The illustration of band gap of QDs depending on their sizes and (B) fluorescence process in a bulk semiconductor [8-11]

Semiconductor quantum dots (QDs) are generally composed of three parts: core, shell and surface coating as shown in **Figure 2.4.**

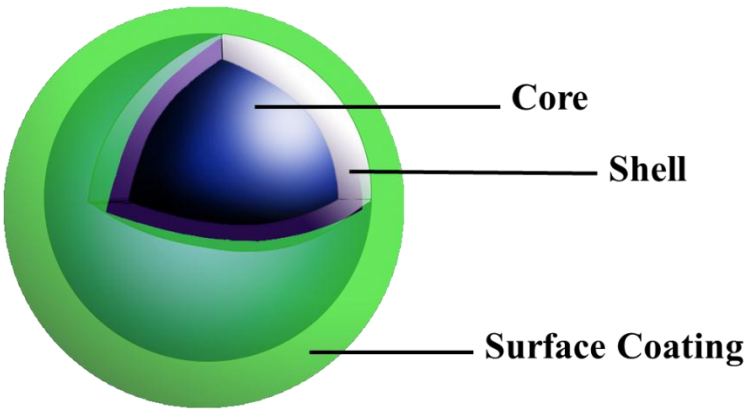

Figure 2.4 The semiconductor quantum dots (QDs) structure

In the first part, core of QDs typically is composed of groups II–VI, III–V, or IV–VI in periodic table such as CdSe, CdS, CdTe, PdSe, and InP. This part influences optical luminescence property the most. Second part is the shell that was coated onto the core surface in order to protect and prevent electrons from getting out of the conduction band that could lead to a decrease in fluorescent emission. The shell significantly improves the fluorescence stability and help against photo-bleaching. The most used shell is ZnS shell because ZnS shell has large band gap comparing to other semiconductors as shown in **Figure 2.5.** For the last part, surface coating is used for improving and assisting the quantum dot nanoparticles to apply in wide applications. The optical property depends on many factors, for instance, size and composition. The size of semiconductor quantum dot nanoparticles significantly affects their optical property. The larger nanoparticle emit in red-shift wavelength whereas the small particle emit in blue-shift fluorescence as described above. The different metal composition nanoparticle as well as synthesis techniques of quantum dots result in different band gap and various fluorescent emissions.

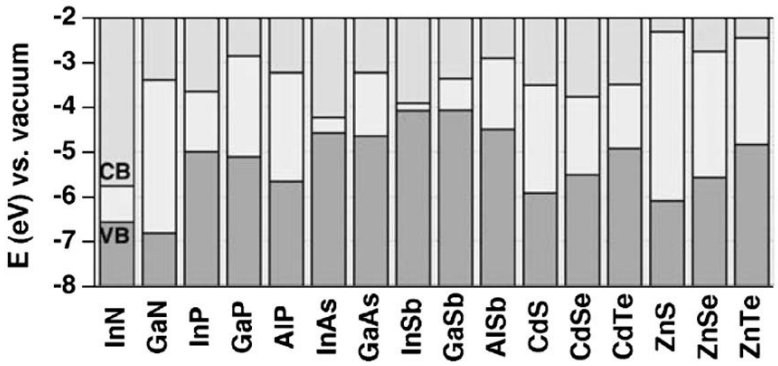

Figure 2.5 Electronic energy levels of semiconductors [12]

For other optical molecules, the similar fluorophores such as fluorescent organic dyes were also used in biological applications. The fluorescent organic dyes are fluorescent chemical compound that can be used as single molecules or conjugation with nanomaterials for used in bio-imaging [3, 13, 14].

In comparison of the properties of quantum dots with other fluorescent organic dyes, QDs display better optical properties than fluorescent organic dyes in that QDs have wide absorbance wavelengths and emission of multiple colors by excitation wavelength of a single light source. On the other hand, fluorescent organic dyes display only one color from one component (**Figure 2.6**). Different organic dye molecules require different excitation energy, so it not suitable for multicolor imaging applications [15]. Other fluorescent characters of QD are that they have high photoluminescence and narrow emission spectrum (narrow FWHM and size) comparing to organic dyes. QD also have better photostability that can enable the use in continuous observation as in bio-labeling application. Moreover, QDs have tunable luminescence and longer fluorescence lifetimes than organic dyes. On the contrary, organic dyes generally have many problem such as broad emission spectrum, overlaping with other emission spectrum easily, photobleaching and excitation changing in different chemical environments [16-19].

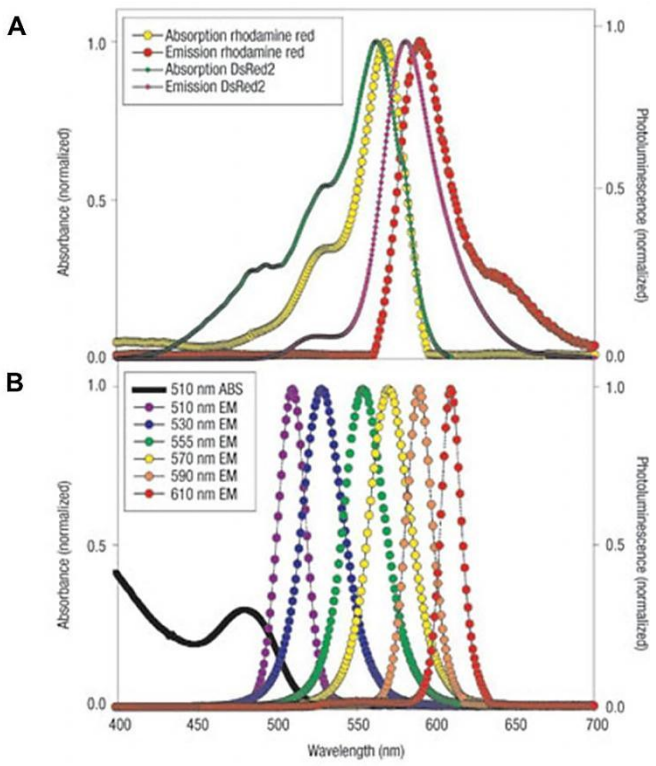

Figure 2.6 The comparison of optical properties between organic dyes (A) to quantum dots (B) [20]

The widely used QDs are cadmium-based QDs such as CdSe, CdS, and CdTe QDs that include heavy metals in the core of QDs, so they inherit with toxicity and environmental impacts as has been reported previously such as in **Figure 2.7** In order to response to the concern and reduce toxicity problem for used in biological applications [21-24], in this work QDs were synthesized using different compositions of non-heavy metal-based core. Zinc-based QDs or ZnSe/ZnS QDs were chosen to be investigated in this research.

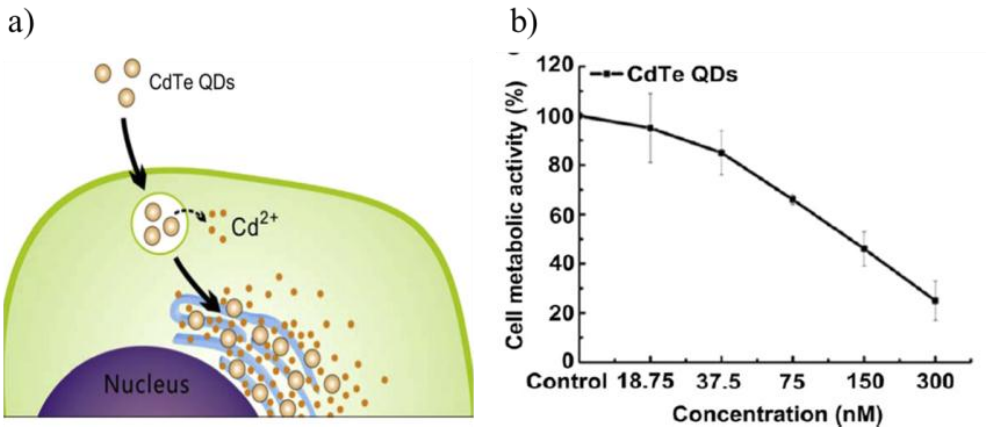

Figure 2.7 Cytotoxicity of CdTe QDs was investigated as a) free cadmium ions from CdTe QD nanoparticles were released into the cytoplasm resulting in b) the decreasing of viable cells [25].

2.2 Zinc-based QDs

The ZnSe/ZnS QDs are semiconductor quantum dots (QDs) consisting of ZnSe core and coated with ZnS as shell. Zinc selenide (ZnSe) semiconductors quantum dots are in the groups II–VI compound with low toxicity and synthesized using environmentally friendly technologies. ZnSe QDs have a wide band gap of 2.7 eV (460 nm) and have a small particle, so their fluorescence falls in violet to blue emission [12, 26, 27]. The superior properties of ZnSe QDs are very narrow emission peaks, high-quality photoluminescence and tunable blue-ultraviolet (UV) luminescence [18]. Therefore, ZnSe QDs have been used in various applications such as in optoelectronic light device applications, i.e. laser diodes, light emitting devices (LEDs), solar cells and bioapplication i.e. sensors, bioimaging and biolabeling [18, 28-30]. Most binary octet semiconductors crystallize either in the cubic zinc-blende (ZB) or in the hexagonal wurtzite (W) structure as shown in **Figure 2.8**, both of which vary in the layer stacking along (111), showing an ABCABC or an ABAB sequence, respectively [31, 32]. ZnSe QDs can adopt both zinc-blende (ZB) and wurtzite (W) structures or they can be called W–ZB polytypism depending on the experimental conditions, nucleation and growth of the nanoparticles [8].

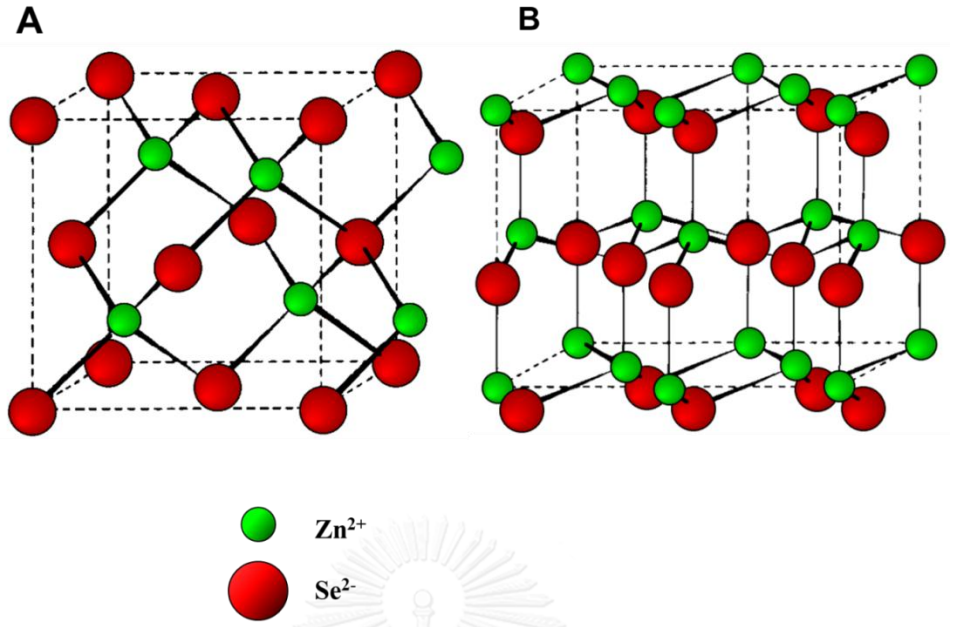

Figure 2.8 The crystal structures of ZnSe QDs (A) zinc blende (ZB) and (B) wurtzite (W) structures [31]

In this research we synthesized ZnSe/ZnS QDs using hot-injection method in organic phase. In hot-injection method, the precursors are injected rapidly into hot solvent. The nanoparticles are produced as nucleation form and undergo growth processes. We used zinc-fatty acid salts as zinc precursors and used trioctylphosphine (TOP) and stearic acid a stabilizing ligand dissolved in 1-octadecene (ODE). The sizes of ZnSe/ZnS rely on the growth temperature and time. The synthesized ZnSe/ZnS QDs by hot-injection method have high photofluorescence stability and good dispersibility. ZnSe/ZnS QDs were surrounded by hydrophobic ligand, which were used to control the sizes of the QDs during the synthesis, but it allow the QDs to only dissolve in organic solvent. Therefore, the as-synthesized QDs only disperse in organic solvent. In order to improve solubility and transfer QDs into aqueous phase for biological application, QDs need to have hydrophilic ligands on their surface.

2.3 Surface modification of nanoparticles

In order to apply in biological applications, QDs nanoparticles have to be dispersed in water or aqueous phase. However, many QDs nanoparticles usually

disperse in organic solvent such as hexane, chloroform and toluene because their surface is coated with hydrophobic ligands. QDs nanoparticles need to have hydrophilic ligands on their surface. Therefore, we aim at modifying the surface of QDs. The methods of surface modification can be classified into several processes. However, the well-known and widely used are two main strategies: ligand exchange and encapsulation.

2.3.1 The Surface modification strategies

2.3.1.1 Encapsulation method

In this method, amphiphilic molecule polymers are used to encapsulate to nanoparticles without replacing the original ligands on their surface. (**Figure 2.9**) The encapsulated nanoparticles are normally in micellar formation that can be dispersed in water solution. This method helps balance the hydrophobic and hydrophilic of ligand due to a non-polar part of polymer will enclose hydrophobic inside, whereas a polar head of polymer is outside to functionalize and assist in water dispersibility. The widely used amphiphilic polymers are such as phospholipids and polymethylacrylic acid. Drawback of this method is that polymer-encapsulated QDs can be notoriously difficult to functionalize. Moreover, the encapsulated nanoparticles have large hydrodynamic diameters leading to a decrease biocompatibility [33].

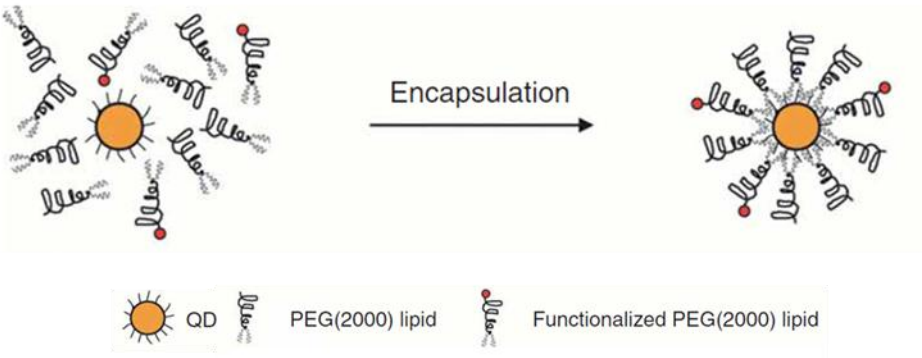

Figure 2.9 Diagram illustrating the surface modification of QDs using encapsulation method [34]

2.3.1.2 Ligand exchange method

One of the most used method for surface modification of nanoparticles is ligand exchange method or cap exchange method. Concept of ligand exchange is to replace the original ligands on nanoparticle surface with new ligands that could improve dispersibility of nanoparticles in aqueous media as shown in **Figure 2.10.** Hydrophilic ligands do not only play their role in dispersibility in aqueous phase, but they can also be chemically functionalized with the terminal functional groups to serve for various applications (**Figure 2.11**). Moreover, the ligand molecule can stabilize the nanoparticles in aqueous phase. The used ligands should have strong affinity for the atoms at the QDs surface such as thiol group in order to bind tightly to the QD surfaces and can thus easily replace the original surfactant molecules. The ligand exchange method has many advantages. For instance, it gives the particles with small hydrodynamic diameters, and some ligands can be easily manipulated at molecular level.

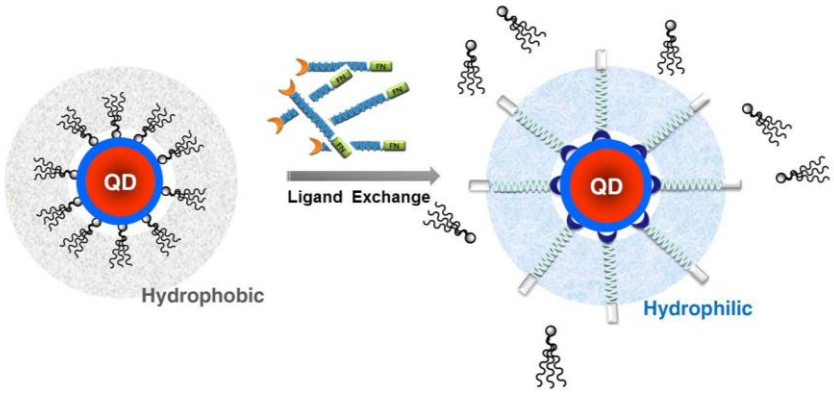

Figure 2.10 Diagram illustrating the surface modification of QDs using ligand exchange method [35]

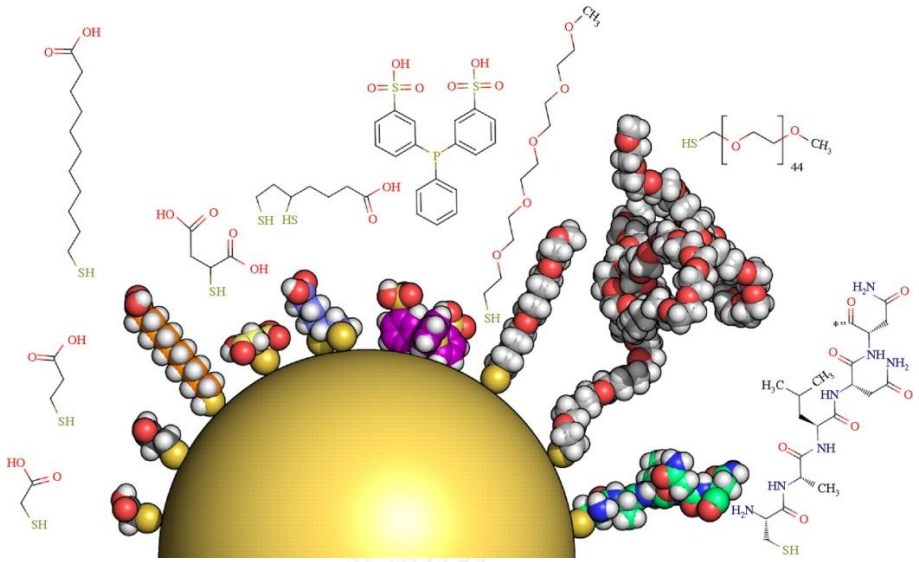

Figure 2.11 The illustration of nanoparticle conjugated with the different hydrophilic ligand [36]

Hydrophilic ligands have a role in improving dispersibility in aqueous phase. Furthermore, they can be chemically functionalized with the terminal functional groups to serve for various applications. It has been reported that thiol ligands are ligands with great potential for development as they can strongly bind with metal on the QDs surface. The thiol ligand bonds onto the inorganic surface by coordination bond based on Lewis acid/base interactions; moreover, the terminal functional group of thiol ligand (such as carboxylic acids or amino acids) can promote affinity to aqueous solutions [35].

Dihydrolipoic acid (DHLA) ligand is a common dithiol ligand that has carboxylic acid as the terminal functional group. Dihydrolipoic acid (DHLA) is a reduced disulfide bond form of thiotic acid with structure shown in **Figure 2.12**

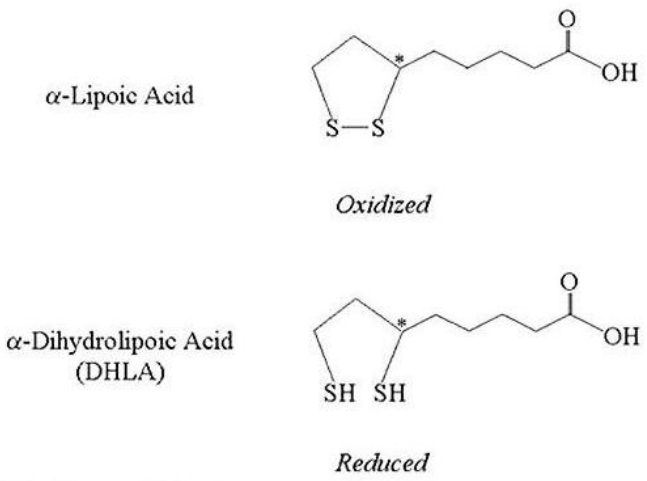

Figure 2.12 Chemical structures of thiotic acid (TA) and dihydrolipoic acid (DHLA) ligand [37]

Another promising dithiol ligand is 4-(3,5-bis(mercaptomethyl)phenoxy) butanoic acid (BMPBA) (**Figure 2.13)** as a single aromatic ring between thiol groups has been proposed to prevent thiol group from forming a disulfide bond and increase the stability of QDs after ligand exchange [38, 39].

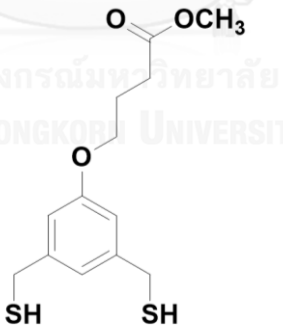

Figure 2.13 The structures of 4-(3,5-bis(mercaptomethyl)phenoxy) butanoic acid (BMPBA)

In order to increase water dispersibility and biocompatibility of the nanoparticles, polymer coating is one of important methods used in various applications.

2.3.2 Polymer coating

To apply in biological applications, the surface modification uses hydrophilic molecule in combination with polymer to coat on nanoparticles to assist in their water-dispersibiliy. The polymer used in many biological applications must concern about biocompatible, dispersibility and low toxicity. The benefits of this functionalized QDs nanoparticles are that the polymer could assist in QDs stability and reduce effects of the environment on the optical properties of QDs.

2.3.2.1 Poly(amidoamine) dendrimers

Dendrimers are macromolecules with highly branched structure that have ubiquitous dendritic patterns, unique interfacial and functional performance advantages in the biomedical applications; for instance, stability of molecule, monodispersion, high capacity for drug delivery and high surface functionalities. Dendrimers are known as starburst polymer.

Poly(amidoamine) or PAMAM dendrimers are one of the well-known dendrimers polymer that have unique properties. Moreover, they were interesting when compared to other classes of dendrimers in biomedical applications. The use of PAMAM has abundant advantages; for instant, PAMAM is biocompatible, soluble in aqueous solution and water, shows low cytotoxicity, contains multiple conjugate functional groups such as amine, carboxyl, and hydroxyl for various biomolecule linkages [40], leading to bind various target molecules such as antibodies, proteins or become special carrier systems for specific genes and drugs delivery. In addition, PAMAM polymer were used as mimicry globular proteins or artificial proteins due to its systematic dimensional, length, scaling, and other biomimetic properties [41, 42].

In 1985, for the first time, Tomalia and coworkers successfully synthesized, characterized and commercialized the complete PAMAM dendrimers family [43]. Structure of PAMAM dendrimers consists of a core, branching units and terminal surface groups as shown in **Figure 2.14.**

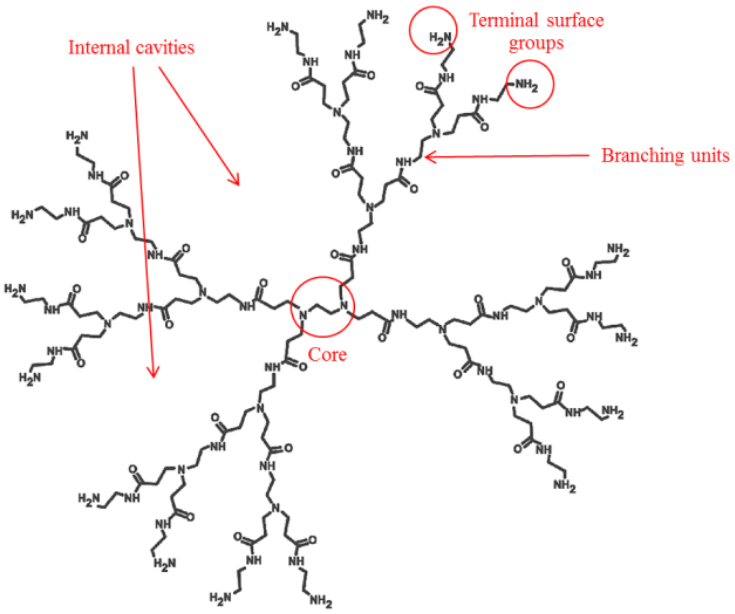

Figure 2.14 Structure of PAMAM polymer [41]

Syntheses of PAMAM can be done using two principle strategies 1) divergent method and 2) convergent method as shown in **Figure 2.15**. PAMAM dendrimers can be mostly synthesized by divergent method. In the divergent method, dendrimer grows directly from a core site and proceeds radially outwards with stepwise addition of successive layers of building blocks. On the other hand, convergent method, dendrimer growth begins from the final macromolecule and proceeds inwards.

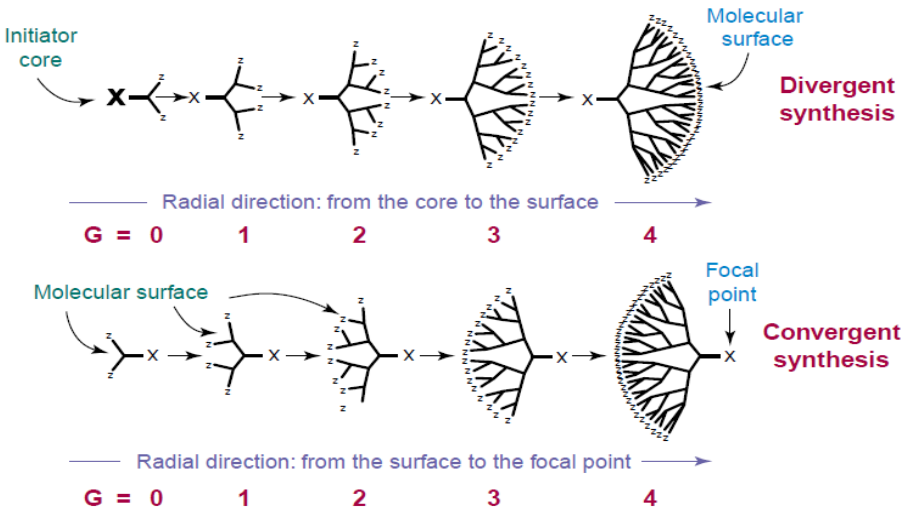

Figure 2.15 Scheme for two principle synthetic methods for dendritic macromolecules the divergent method and the convergent method [44]

In the synthesis of PAMAM dendrimers, ethylenediamine was used as core to start amidation reaction on its amino groups with methyl acrylate following by Michael addition method as shown in **Figure 2.16** At a result, PAMAM dendrimers consist of alkyl-diamine core and tertiary amine branches, in the available range from 10 – 130 Å in diameter for generation G0 through G10 with five different core types and ten different functional surface groups [44] as shown **in Figure 2.17 and Table 2.1.**

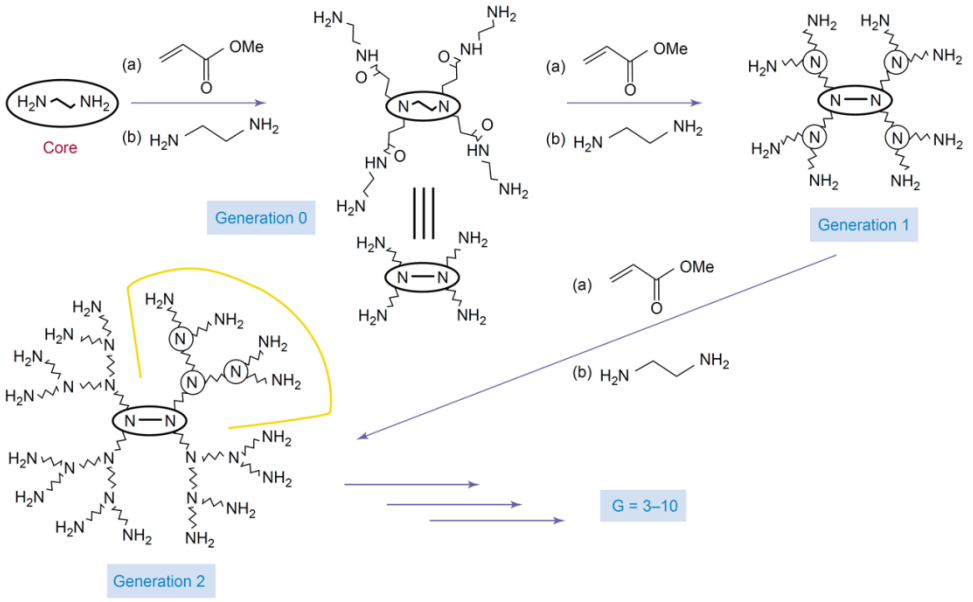

Figure 2.16 The scheme for the synthesis of PAMAM polymer dendrimers [44]

Table 2.1 The calculated properties of primary amine surface functional group of PAMAM dendrimers according to their generation and common alternative surfaces [45].

Generation	Molecular Weight	Measured Diameter (Å)	Surface Groups
0	517	15	4
1	1,430	22	8
2	3,256	29	16
3	6,909	36	32
4	14,215	45	64
5	28,826	54	128
6	58,048	67	256
7	116,493	81	512
8	233,383	97	1024
9	467,162	114	2048
10	934,720	135	4096

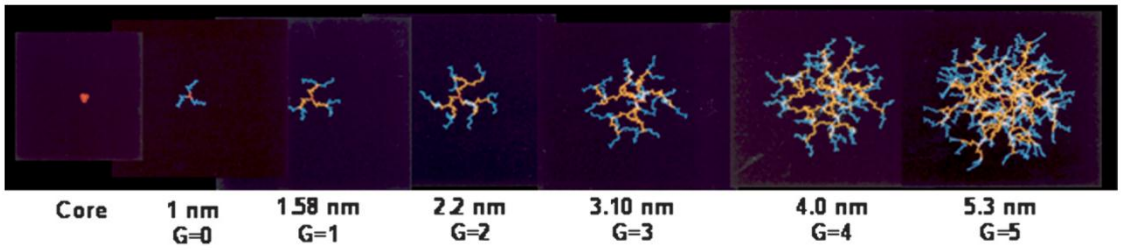

Figure 2.17 The structures of example generation of PAMAM polymer dendrimers [46]

In this research we focus on using ligand exchange to modify the surface of QDs by using dithiol ligands that acts as an anchor group with carboxylic acid terminal group**.** The modified QDs were then conjugated with PAMAM in order to improve QDs to become biocompatible and low toxicity for applying in biological applications.

2.4 MTT assay and cytotoxicity studies

The MTT (3-[4,5-dimethylthiazol-2-yl]-2,5 diphenyl tetrazolium bromide) assay is used to measure cell viability calculated from conversion of tetrazolium salt MTT into formazan crystals form by living cells (**Figure 2.18**). MTT assay is the most common method to determine cytotoxicity of drugs or nanoparticles for *in vitro* study. Mitochondrial activity of living cells has important role as it can convert a yellow color tetrazolium MTT to a reduction form of purple formazan crystals by *mitochondrial reductase* enzymes released from living cells. When the purple formazan crystals were dissolved, its concentration was measured by a spectrophotometer. Therefore, increase or decrease of viable cells can be calculated as the number of live cells.

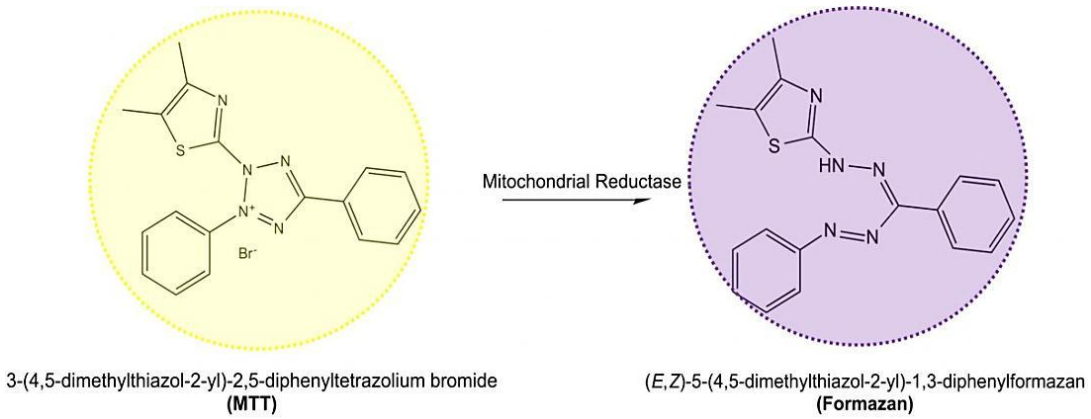

Figure 2.18 The reaction of MTT with mitrochondria reductase from living cells that transform MTT to formazan form

2.5 Literature reviews

2.5.1 Syntheses and applications of ZnSe/ZnS QDs

Many researchers studied and synthesized ZnSe/ZnS QDs to substitute for CdSe/ZnS QDs in order to reduce toxicity and environmental impacts. For examples;

In 2004, Reiss P. and coworker studied about the size-dependent and optical properties of ZnSe QDs by the hot-injection method using the non-coordinating solvent 1-octadecane. They found that the photoluminescence of the QDs showed an extremely narrow peak in the spectral range of 390–440 nm with constant emission peak widths of 15 nm [47].

Ippen, C. and coworker in 2014 synthesized ZnSe/ZnS quantum dots used in cadmium-free blue QD-LEDs devices. Their QDs emission wavelength can be tuned in range from 390 to 435 nm. Furthermore, ZnSe/ZnS QDs were with color purity, high photoluminescence and narrow emission peak with FWHM of 16 nm [27]. **Figure 2.19** showed the precursors used and the synthesis of ZnSe/ZnS QDs.

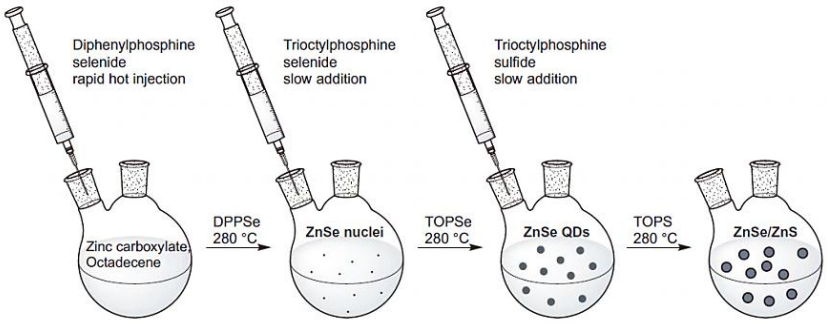

Figure 2.19 The example of synthesis process for ZnSe/ZnS QDs reported by Ippen, C. *et al.* [27]

In 2015 Wang, A. *et al.* synthesized Cd-free quantum dot as ZnSe/ZnS QDs for using in light-emitting diodes (QD-LEDs) application. They were synthesized by a new method namely low temperature injection and high temperature growth. Zinc fatty acid salts and 1-octadecene (ODE) was used as Zn precursors and solvent, respectively. The ZnSe/ZnS QDs displayed violet-blue emission that had tunable wavelengths from 400 to 455 nm. Their synthesis gave QDs with high stability, narrow emission peak (FWHM <20) and photoluminescence quantum yields (QYs) up to 83%, and also successfully demonstrated high quality for apply in LED application [48].

From many literature reviews, ZnSe/ZnS QDs not only can efficiently substitute the use of CdSe/ZnS, but ZnSe/ZnS QDs, but also have good optical property similar to CdSe/ZnS. Therefore, we are interested in the synthesis of ZnSe/ZnS QDs that use the non-coordinating solvent 1-octadecane and zinc complex (zinc fatty acid salts) as precursor by hot-injection method.

2.5.2 Surface modification of QDs with thiol ligand

Thomas Pons and coworker, in 2007 synthesized a ligand by using DHLA as anchor conjugated with poly(ethylene glycol) (PEG) that coupled with various functional terminal groups (biotin, carboxyl, and amine) to modified onto the surface of CdSe/ZnS QDs that were shown in **Figure 2.20.** The modified ligand can improve water-dispersibility and biocompatibility of QDs. The surface of QDs were modified

using a cap exchange method with their modified ligand. Moreover, they studied about biochemical conjugation, and they found that the QDs with DHLA-PEG ligand can effectively conjugate with biomolecules such as with NeutrAvidin, streptavidin in live cells [49].

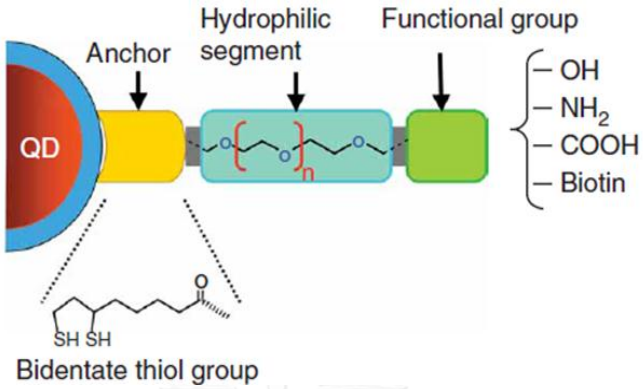

Figure 2.20 The illustration of QDs modified with hydrophilic ligands and various terminal functional groups [49]

In 2007 W. Liu, *et al.* synthesized CdSe(ZnCdS) QDs coated with cysteine by using ligand exchange and transferred the QDs from organic to aqueous phase (**Figure 2.21**). The QDs-Cysteine dispersed in PBS buffer at pH 7.4. The fluorescence of CdSe(ZnCdS)QDs slightly dropped from around 66% to 40% in water. They obtained high fluorescent, biocompatible, low toxic and easy functionalized QDs for bio-imaging [50].

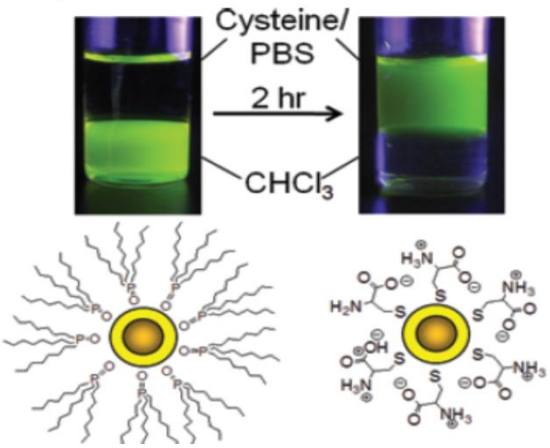

Figure 2.21 Photographs and proposed structures of QDs before and after ligand exchange with DL-cysteine [50]

In 2013 Lee, H.J. and coworker designed and synthesized the new carboxylic acid-terminated alkanethiol having bidentate character that were 16-(3,5-bis(mercaptomethyl)-phenoxy)hexadecanoic acid (BMPHA) with the structure as shown in **Figure 2.22**. BMPHA was coated onto gold nanoparticles using self-assembled monolayers method (SAM). They studied about thermal stability of BMPHA ligand compared to those derived from mercaptohexadecanoic acid (MHA) and 16-(4-(mercaptomethyl)phenoxy)hexadecanoic acid (MMPHA) as shown in **Figure 2.22**. Thiol ligands that have phenyl-incorporating thiols with a single methylene spacer were better ordered than thiols directly attached to the aromatic ring because the aromatic ring and the spacer prevented a formation disulfide bond from the dithiols. Therefore, BMPHA were more stable in both nonpolar and polar protic solvents even when heated up to 90°C comparing to MMPHA and MHA [38].

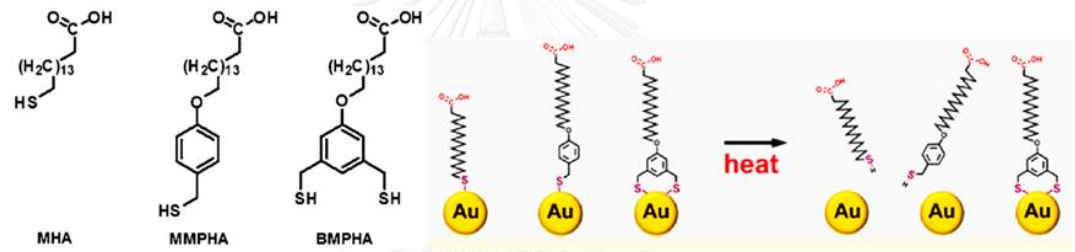

Figure 2.22 The carboxylic acid-terminated bidentate alkanethiol ligand of this research [38]

2.5.3 Surface modification of nanoparticles with PAMAM polymer

In 2010, Zhao, Y. and coworker designed and synthesized CdSe/ZnS quantum dots that functionalized with folate–poly(ethylene glycol)–polyamidoamine (FPP) for the optical detection of tumor cells. Ligand-exchange method was used for the conjugation between QDs to FPP ligand. The modified QDs were hydrophilic and stable in water solution. They found that QDs coated with FPP can target and detect tumor cells successfully by folate receptor recognition as shown in **Figure 2.23** [51].

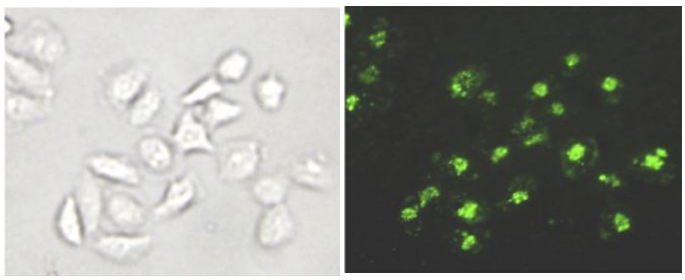

Figure 2.23 The photographs of cellular uptake of QDs-FPP in HeLa cells: (left) phase contrast images and (right) fluorescence image [51].

Then in 2011, Higuchi, Y *et al.* modified commercial QDs with PAMAM dendrimer to promote the uptake of QDs into mesenchymal stem cells (MSCs) through electrostatic interaction. The uptake efficiency of QDs in MSCs were increased by the modification of the PAMAM dendrimers. Moreover, PAMAM helps prolong the intracellular fluorescence intensity [52].

In 2014, Figueroa, E.R. *et al.* synthesized and developed gold nanoparticle (AuNPs) conjugated with PAMAM dendrimers by EDC coupling method for use as non-viral transfection agents for gene therapy. The gold nanoparticles were coated with 11-mercaptoundecanoic acid (MUA) as thiol anchor and were conjugated PAMAM dendrimers via EDC and sulfo-NHS. AuNPs-PAMAM showed high transfection efficiency, stability and low cytotoxicity [53].

From literature reviews, many researchers synthesized and modified nanoparticles by ligand exchange method using only thiol ligand or dithiol ligand to conjugate with various biomolecule. In this work, we are interested in modifying the surface of ZnSe/ZnS QDs using ligand exchange method, and the dithiol ligand is chosen as anchor due to strong binding onto ZnSe/ZnS QDs surface. The dithiol anchor ligands were conjugated with PAMAM dendrimers to improve biocompatible and dispersibility before the investigation of the biocompatibility of the modified nanoparticles.

CHAPTER III

EXPERIMENTS

3.1 Instruments

1. Ultraviolet-visible spectroscopy (UV-Vis spectroscopy, Agilent 8453)
1. Fluorescence spectroscopy (Varian Cary eclipse fluorescence spectrophotometer)
2. Transmission electron microscope (TEM, JOEL, JEM-2100)
3. Fourier-transform infrared spectroscopy (FT-IR, Nicolet, Impact 410)
4. Proton-Nuclear magnetic resonance (^{1}H-NMR, Bruker 400 MHz.)
5. X-ray powder diffraction spectrometer (XRD, Rigaku, DMAX2200/Ultima+)

3.2 Chemicals

1. Zinc stearate, ZnO 12.5-14% (Alfa Aesar)
2. Thiotic acid, TA (Alfa Aesar)
3. Zinc acetate dehydrate, $Zn(CH3COO)_2 \cdot 2H_2O$ 98% (Aldrich)
4. Selenium, Se 99.99% (Aldrich)
5. Sulfur, S 99.98% (Aldrich)
6. 1-Octadecene, ODE 90% (Aldrich)
7. Trioctylphosphine, TOP 97% (Aldrich)
8. Hexadecylamine, HDA (Aldrich)
9. Trioctylamine, 98% (Aldrich)
10. PAMAM dendrimer G0, ethylenediamine core, 20 wt. % in methanol (Aldrich)
11. Ethylenediamine, EDA 99% (Aldrich)
12. N-(3-Dimethylaminopropyl)-N′-ethylcarbodiimide hydrochloride, EDC (Chem-Impex)
13. N-Hydroxysuccinimide, NHS 98% (Aldrich)
14. 4-(Dimethylamino)pyridine, DMAP (Aldrich)

15. N,N′-Dicyclohexylcarbodiimide, DCC (Aldrich)
16. Sodium borohydride, $NaBH_4$ (Aldrich)
17. Ellman's reagent or 5,5'-dithiobis-(2-nitrobenzoic acid), DTNB (fisher chemical)
18. Hexane, AR grade (RCI Labscan)
19. Ethanol, AR grade (RCI Labscan)
20. Acetone, AR grade (RCI Labscan)
21. Chloroform, AR grade (RCI Labscan)

3.3 Synthesis of ZnSe/ZnS quantum dots

The ZnSe/ZnS core/shell nanoparticles were synthesized by a hot-injection method using zinc precursor (zinc fatty acid salts) dissolved in 1-octadecene as a non-coordinating solvent in one pot. The synthesis was divided into 3 following steps.

3.3.1 Preparation of Zn precursor

0.21 g zinc acetate dihydrate and 1.6 g HDA were stirred in 5 mL trioctylamine under vacuum for 1 h before used.

3.3.2 Preparation of Se precursor

Stock solution of selenium precursor (TOPSe 1 M 40 mL) was prepared by dissolving 3.162 g selenium powder in 40 mL TOP under nitrogen gas and was stirred overnight to obtain clear colorless solution.

3.3.3 Preparation of S precursor (TOPS)

Sulfur precursor (TOPS 2 mmol 5 mL) was prepared by dissolving 0.0641 g sulfur powder in TOP 5 mL under nitrogen gas and was stirred to obtain clear colorless solution.

For the synthesis of the QDs, 1.5494 g zinc stearate, 0.97 g hexadecylamine (HDA) and 15 mL 1-octadecene were loaded into a 100 mL three-necked bottle. Then the mixture was heated and stirred at 120 ºC under vacuum for 1 h. After 1 h the light yellow solution was obtained and was heated up to 300 ºC under nitrogen gas. Then, 5 mL Se precursors was injected rapidly at 300 ºC, and the

mixture was maintained at this temperature for 4 min. Next, temperature was cooled down to 70 °C before zinc precursor was injected into the mixture. Then the mixture was heated to 150 °C, and Sulfur precursor (TOPS) was added dropwise to the mixture. Finally, the temperature was cooled down to 60 °C before the ZnSe/ZnS core/shell quantum dots was injected with 10 mL hexane and kept in the vials covered with aluminum foil. The method showed in **Figure 3.**1 with the temperature program used as shown in **Table 3.1**.

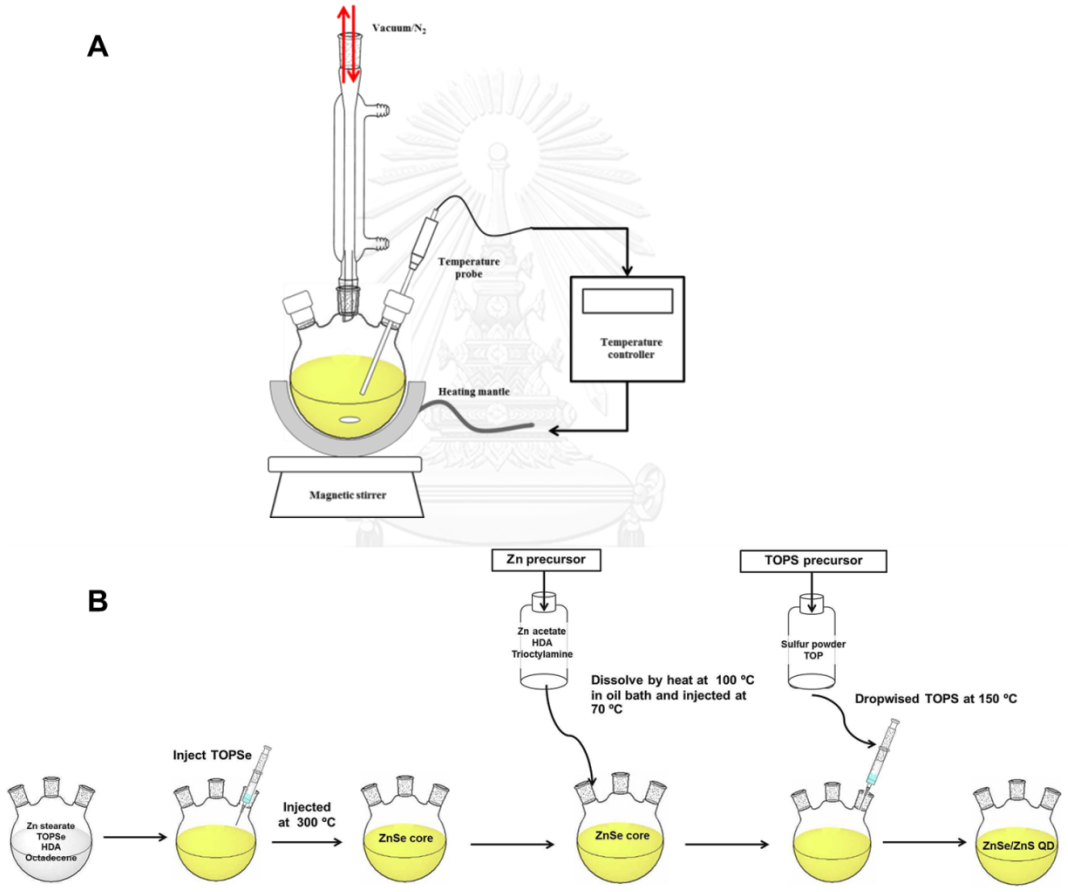

Figure 3.1 Illustration of QDs synthesis setup (A) and scheme of synthesized ZnSe/ZnS quantum dots in one-pot (B)

Table 3.1 Temperature program for the synthesis of ZnSe/ZnS quantum dots in one-pot

Step	Temperature (°C)	Duration (min)	Condition
1	120	5	vacuum
2	120	90	vacuum
3	300	15	under N_2 gas
4	300	4	injected Se precursor (TOPSe) rapidly, under N_2 gas
5	70	5	injected Zn precursor for shell, under N_2 gas
6	150	5	under N_2 gas
7	150	30	dropped S precursor (TOPS), under N_2 gas
8	60	5	under N_2 gas

3.4 Ligand exchange process

3.4.1 Syntheses of thiol ligands for surface modification of QDs

Synthesis of DHLA conjugated with PAMAM was performed according to the synthesis procedures for DHLA preparation and conjugation [54]. 0.6 mmol Thiotic acid (TA), 1 mmol PAMAM, and 0.3 mmol DMAP were dissolved in 20 mL DCM. Then 1 mmol DCC was added into the mixture while stirred at 0 °C for 2.5 h. Next, the mixture was continued stirring at room temperature overnight. DCM was then evaporated from the product. This reaction was shown in **Scheme 3.2.** Then product was dissolved in ethanol and H_2O in ratio 3:1 mL to open ring of disulfide

bond in product by using $NaBH_4$ (product: $NaBH_4$ = 1: 5 mol) [49]. The mixture was stirred at room temperature for 1 h under N_2 gas. Finally, the mixture was extracted with chloroform (5 mL x4 times), evaporated and stored the DHLA-PAMAM product in vial. Another synthesis of ligand BMPBA conjugated with PAMAM, BMPBA was obtained from Lee group at University of Houston according to previous report [38]. In this research, BMPBA ligand was coated onto QDs before conjugation with PAMAM because of limit of BMPBA quantity. This reaction was shown in **Scheme 3.3.** The overall of ligand exchange process is shown in **Scheme 3.1.**

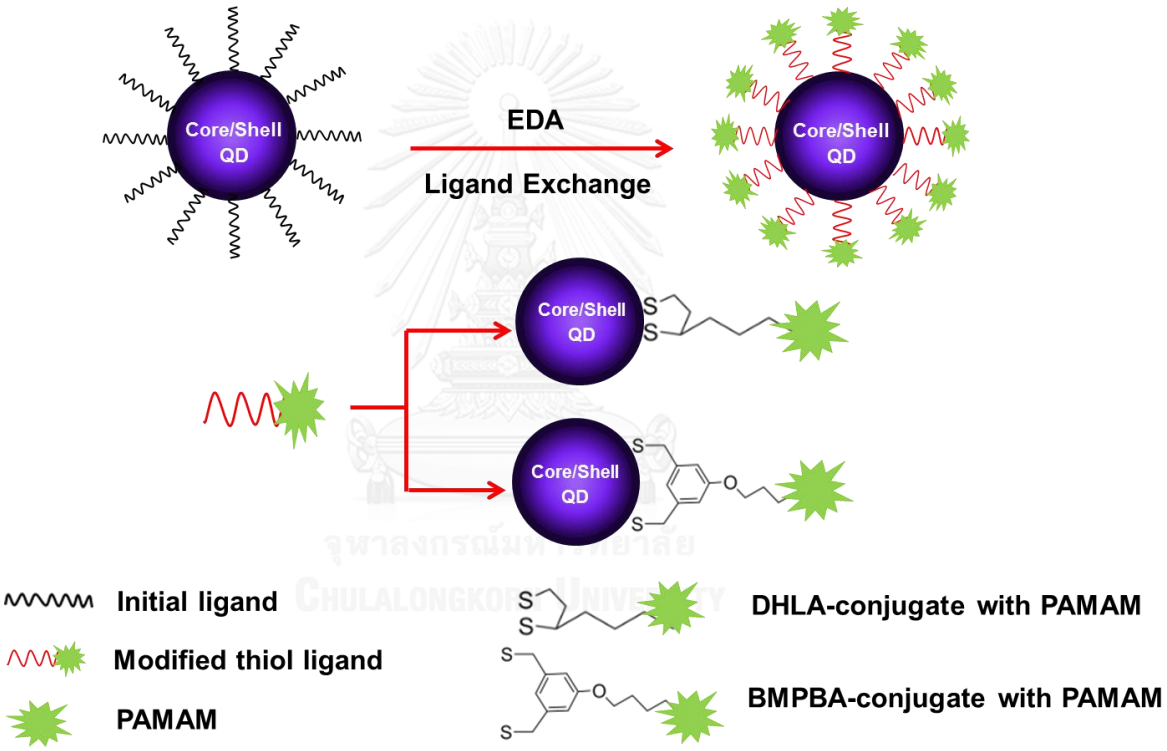

Scheme 3.1 Illustration of ligand exchange of ZnSe/ZnS QDs with thiol-conjugated PAMAM

3.4.2 Conjugation of QDs with modified thiol-PAMAM ligand using ligand exchange method

The surface of ZnSe/ZnS quantum dots were modified using ligand exchange method [55]. Briefly, QDs were precipitated with acetone and methanol.

The precipitated QDs were re-dispersed in 1 mL chloroform, and 0.5 mL EDA was added to the solution under vigorous stirring for 30 min. Then 0.15 M thiol ligand (in 3.4.1) in milli-Q water was added to the mixture solution with stirring for 1 h. After reaction was completed, quantum dots were transferred to the aqueous phase and separated from organic phase. In order to eliminate exceed amine, aqueous phase was washed and adjusted to pH ~8 with milli-Q water and PBS buffer, respectively. Finally, the solution was kept in PBS buffer pH~8.

The modified QDs-thiol solution in 1 mL PBS buffer was added into a vial with vigorous stirring. Excess PAMAM polymer was added into solution. Then, 200 µL (45 mg/mL) EDC was added at room temperature under stirring for 3 h. Excess EDC in product mixture was removed by dialysis centrifuge tube, and the final product was adjusted to pH~8 and kept in PBS buffer.

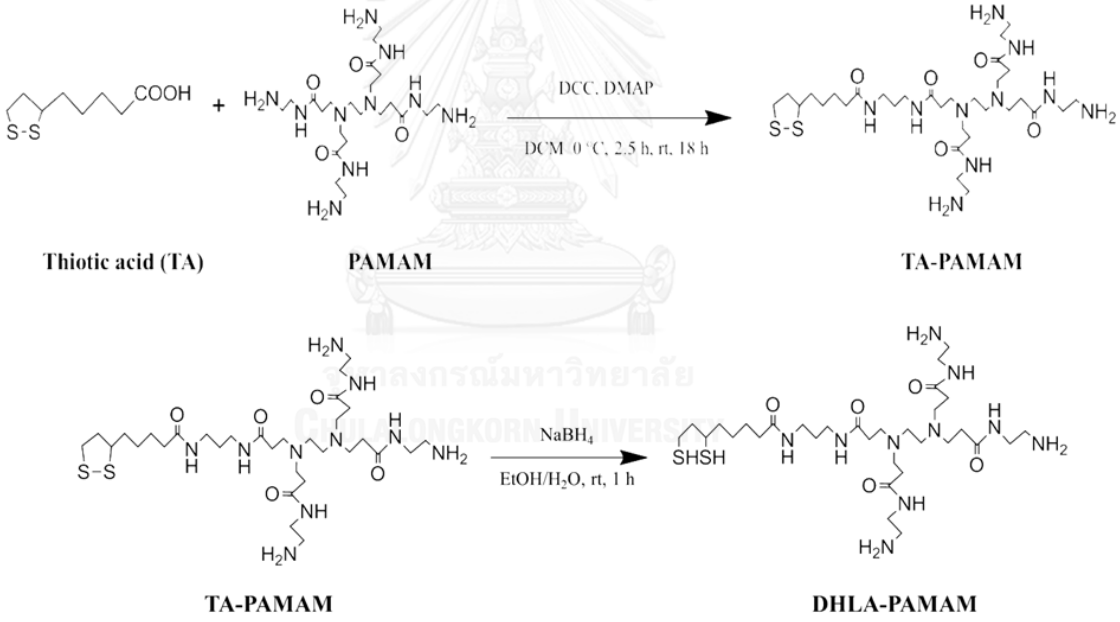

Scheme 3.2 Reaction scheme for conjugations of thioctic acid with PAMAM polymer

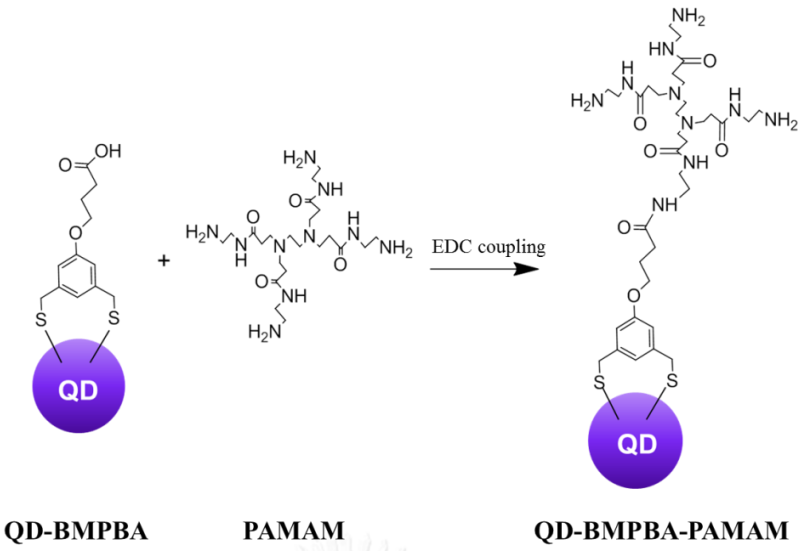

Scheme 3.3 Reaction scheme for conjugations of QD-BMPBA with PAMAM polymer

3.5 Characterization of ZnSe/ZnS QDs

3.5.1 Ultraviolet-visible spectroscopy

The absorption spectra of QDs were characterized using ultraviolet-visible spectroscopy (UV-Vis spectroscopy, Agilent 8453) scanning from the 200 nm to 700 nm at room temperature. The bulk absorption of ZnSe/ZnS QDs at 350 nm was used in the calculation of relative quantum yields of the particles.

3.5.2 Fluorescence spectroscopy

Fluorescence spectroscopy was investigated by Varian Cary Eclipse spectrofluorometer. The emission spectra of the ZnSe/ZnS QDs scanning from 360 nm to 700 nm were recorded with an excitation wavelength at 350 nm at room temperature. The data were used in calculation for relative quantum yields of the QDs.

3.5.3 Transmission electron microscope (TEM)

The morphology of ZnSe/ZnS QDs as size and shape were characterized by Transmission electron microscopy (TEM, JEOL 2100CX, 200 kV microscope). The samples were prepared and deposited by dropping the solution of ZnSe/ZnS QDs in hexane onto a carbon-coated copper grid and were dried at room temperature least for 24 h.

3.5.4 X-ray Powder Diffractrometer (XRD)

X-ray powder diffraction (XRD) analyses were performed using Rigaku D/MaX-2200 Ultima-plus instrument with Cu K radiation (1.5418 A° source (40kV, 30mA)). The precipitated QDs samples were placed on a glass holder. The scans were performed at 25°C in steps of 0.03° over 2-theta ranging from 20° to 80°.

3.5.5 Scanning electron microscopy with energy dispersive X-ray spectroscopy (SEM-EDX)

The dispersive X-ray spectroscopy (EDX) is one of the analytical techniques in SEM or TEM that is used to elemental analysis of materials. ZnSe/ZnS QDs were analyzed composition by SEM-EDX (JEOL, JSM-IT10). The samples were prepared and dried by dropping the solution of ZnSe/ZnS QDs in hexane onto a small silica wafer at room temperature least for 24 h.

3.6 Characterization of ZnSe/ZnS QDs-DHLA-PAMAM and ZnSe/ZnS QDs-BMPBA-PAMAM

3.6.1 Ultraviolet-visible spectroscopy

The absorption spectra of ZnSe/ZnS QDs-DHLA-PAMAM and ZnSe/ZnS QDs-BMPBA-PAMAM QDs were characterized by UV-Vis spectroscopy as the similar aforementioned condition.

3.6.2 Fluorescence spectroscopy

The emission spectra of ZnSe/ZnS QDs-DHLA-PAMAM and ZnSe/ZnS QDs-BMPBA-PAMAM QDs were characterized by Varian Cary Eclipse spectrofluorometer as the similar aforementioned condition.

3.6.3 Fourier-transform infrared spectroscopy (FT-IR)

The QDs-thiol conjugated with PAMAM polymer were characterized using Fourier-transform infrared spectroscopy (FT-IR) performed on an impact 410 (Nicolet). The samples were prepared by mixing with KBr powder and were pressed into a pellet form. The range of frequency was used 400 to 4000 cm^{-1}.

3.6.4 Proton-nuclear magnetic resonance (^{1}H-NMR)

The ligand thiols conjugated with PAMAM were characterized by proton nuclear magnetic resonance (^{1}H-NMR) that were recorded by Bruker NMR spectrometer 400 MHz.

3.7 Cell culture

L929 or mouse fibroblast cell lines were cultured in Dulbecco's modified Eagle's medium (DMEM) supplied with 10% FBS (fetal bovine serum) and 1% antibiotics at 37°C and 5% CO_2.

3.8 Cytotoxicity assay

Cytotoxicity of QDs modified thiol-PAMAM was investigated by measuring the cell viability using the methyl thiazol tetrazolium bromide (MTT) assay. In this research, we used L929 mouse fibroblast cell line as a connective tissue cell line. L929 cells were plated in 96 well-plates with the concentration at 30,000 cells/well in 200 μL DMEM media. Then, cells were incubated at 37°C and 5%CO_2 for 24 h in a humidity hood. Afterwards, the 100 μL of DMEM media was removed and 100 μL of new media was added in each well-plate. Next, the modified thiol-PAMAM of Zn-based QDs (ZnSe/ZnS QDs) were used with concentration from 0 to 0.1 mg/mL in PBS buffer at pH 8 (3 replicates for each concentration in comparison with Cd-based QDs (CdSe/ZnS QDs) with the same coating. CdSe/ZnS QDs that used in this work were synthesized following the method used in our research group [56]. The 20μL MTT solution (12mM, 5mg/mL) was added after 24 h incubation and the mixture solution in 96 well-plates were incubated for 1 h. After incubated with MTT solution, the excess MTT solution was removed by washing with 100 μL of PBS (2 times). Then, the media in mixture solution were removed and 150 μL DMSO were added in order to dissolve the purple formazan crystals. Finally, the absorbance of mixture solution was measured by the Epoch Microplate Spectrophotometer at 570 nm for calculation of percentage of cell viability as shown in the equation below.

$$\% \text{ cell viability} = \frac{A_{sample} - A_{blank}}{A_{control} - A_{blank}} \times 100$$

A_{sample} = Absorbance of sample (cells exposed to nanoparticles)
A_{blank} = Absorbance of media without cells
$A_{control}$ = Absorbance of negative control (untreated cells)

CHAPTER IV
RESULTS AND DISCUSSION

In this chapter, we demonstrate results and discussion that are composed of three main parts. The first part is about the synthesis and characteristic of ZnSe/ZnS QD nanoparticles. Second part includes ligands of thiol conjugated with PAMAM which were coated onto QDs by ligand exchange method for ZnSe/ZnS QDs modification. The final part is study of cytotoxicity of ZnSe/ZnS QDs modified with thiol-PAMAM that was investigated by MTT assay.

4.1 Synthesis and characterization of the ZnSe/ZnS QDs

In this work, we have studied the synthesis of ZnSe/ZnS core/shell QDs nanoparticles using Zn complexes as Zn precursor, TOP and HDA as surfactant and using 1-octadecene as solvent by a hot-injection method. We have studied factors affecting to optical property of ZnSe/ZnS QD nanoparticles by varying reaction time, ratio of starting materials and temperature to find the optimized condition that lead to QDs with good photofluorescence. The optical properties were characterized by UV-visible absorption and fluorescence spectroscopy.

We synthesized QDs nanoparticles and studied the parameter affecting the properties of the resulted QDs by varying time for holding the injection temperature after the injection of Se precursor (TOPSe) in the step of synthesis of ZnSe core QDs. The different holding times studied were 0 min (rapidly allowing cooling down after injection), 2, 4, 10, 20 and 30 min at 300 ºC with the molar ratio of Zn:Se = 1:2. The results showed that the reaction produced multiple sizes of nuclei at 0-4 min. Until at 10 min, the fluoresce peak became maximized, and the ZnSe nuclei grew and formed into nanoparticles with highest fluorescent intensity and narrow size distribution observed as fluorescence peak with narrow full width at half-maximum (FWHM). The intensity of fluorescence peak decreased continuously when the holding time went beyond 10 minutes (**Figure 4.1**). Decreasing of fluorescent intensity might be due to the aggregation from the overgrowth of particles.

Therefore, we determined to control the holding time for 10 minutes as the most suitable reaction time.

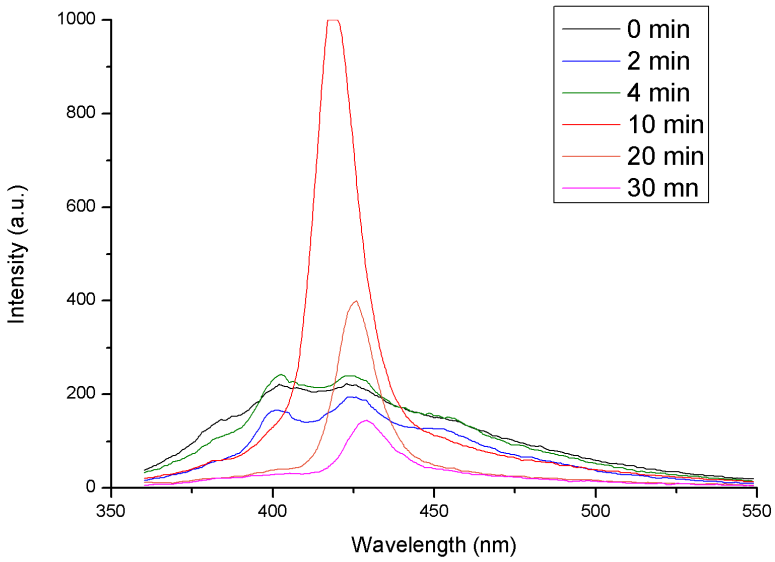

Figure 4.1 PL spectra of QDs nanoparticles from different holding times at the injection temperature.

For the result of injection temperature, the precursor injection was performed at 260, 280, 300, 320 and 340 °C. From the optimized holding time mentioned earlier, we synthesized the ZnSe QDs using holding time of 4 min, or total reaction time of 10 min with Zn:Se molar ratio of 1:2 as the process described in **Section 3.3.** The resulted emission peak at 300 °C showed the highest intensity followed by that of the QDs synthesized at 280 °C as shown in **Figure 4.2.** This observation indicated that the synthesis temperature at 300 °C gave appropriate rate for particle growth resulting in QDs with highest fluorescence.

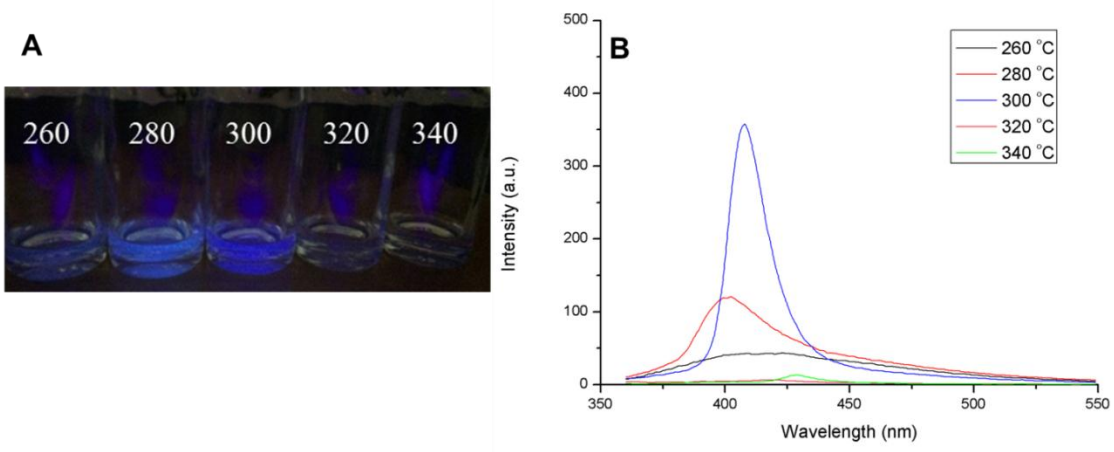

Figure 4.2 (A) Photograph of QD nanoparticles of different temperature under a black light lamp and (B) PL spectra of the QD samples in (A)

Then, we varied the ratio of Zn and Se precursor with Zn:Se molar ratio of 2.5:2.5, 2.5:5.0 and 2.5:7.5 mmol (1:1, 1:2 and 1:3 by mole, respectively). ZnSe QDs were synthesized at 300 ºC and maintained at this temperature for 10 min. The results exhibited that at the ratio of Zn:Se of 1:2, the resulted QD nanoparticles showed highest fluorescent emission peak when compared with other conditions at similar absorbance and the same condition of synthesis (**Figure 4.3**). It indicated that at 300 ºC QDs with Zn:Se of 1:2 can be formed better than QDs from Zn:Se ratio of 1:1 and 1:3. At the ratio of 1:1, growth times might be too short so particle did not grow enough to have high quality photoluminescence. In contrast, at the ratio of 1:3, concentration of Se precursor was too high and affected the uniform particle growth [57].

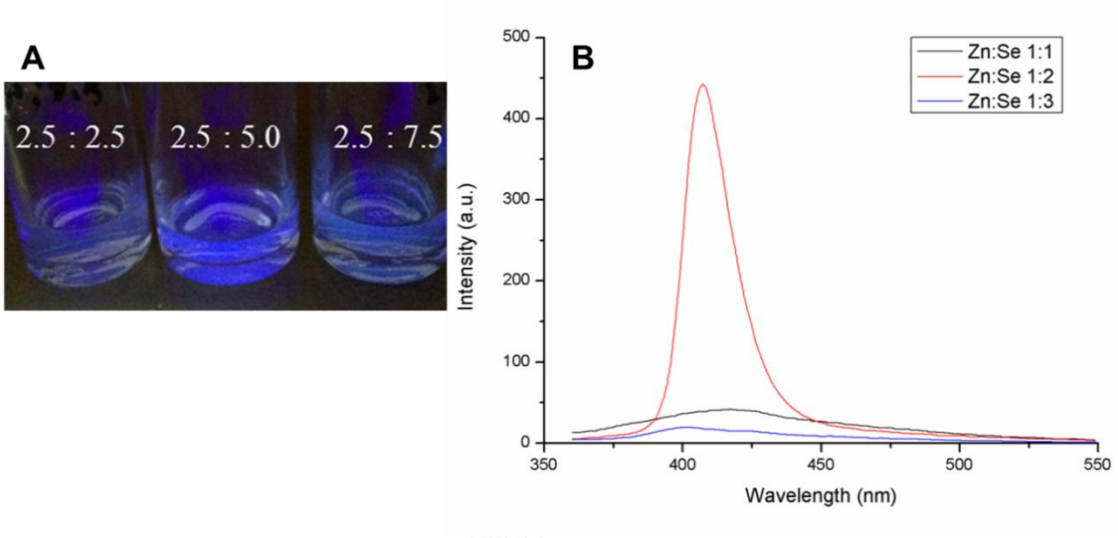

Figure 4.3 (A) Photograph of QDs nanoparticles of different mole ratios under a black light lamp and (B) PL spectra of the QDs samples in (A)

Using the optimal condition for the synthesis of ZnSe core QDs, ZnSe/ZnS core/shell nanoparticles were then synthesized by hot injection method with TOP, HDA and stearic acid as stabilizing in 1-octadexane as non-coordinate solvent. ZnSe/ZnS QDs were prepared by synthesis ZnSe core and ZnS shell QD in a one-pot reaction. ZnSe core nanoparticles were synthesized at 300 °C and without purification, the cores were coated with ZnS shell at 150 °C. The ZnSe/ZnS QDs were characterized for their optical property using UV-visible spectroscopy and fluorescence spectroscopy as shown **in Figure 4.4.** The ZnSe/ZnS QDs exhibited the first absorption peak at 350 nm. Consequently, ZnSe/ZnS QDs emitted a violet-blue light photoluminescence with the maximum wavelength at 410 nm. Moreover, fluorescent emission peaks of ZnSe/ZnS QDs displayed nearly narrow full width at half maximum (FWHM) of 20-30 nm, indicating that ZnSe/ZnS QDs were narrow size distribution. The relative fluorescent quantum yield of ZnSe/ZnS core/shell were calculated as about two folds increase from the ZnSe core.

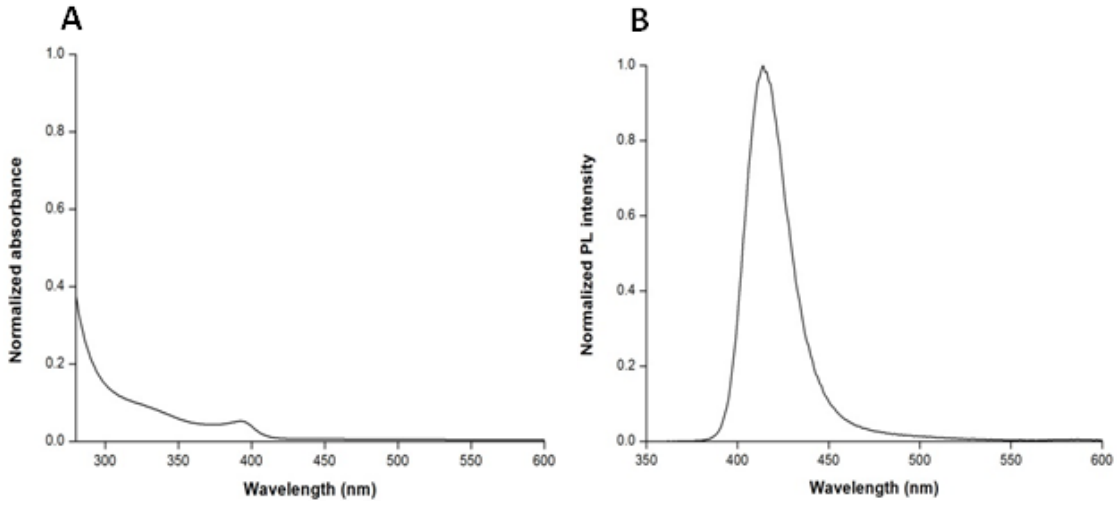

Figure 4.4 Absorption (A) and PL spectra (B) of ZnSe/ZnS QD.

The physical properties of the resulted nanoparticles were characterized using X-ray powder diffraction (XRD), TEM and SEM-EDX. XRD was used to identify crystal structure of QDs nanocrystals. **In Figure 4.5,** the XRD pattern of ZnSe/ZnS core/shell QDs are similar to ZnSe with wurtzite crystal structure. However, there are some peaks showing the presence of impurity attributed to zinc stearate that was used as a precursor. Due to the presence of impurity, signals of ZnS cannot be clearly observed. Therefore, other techniques are required for further confirmation that the core/shell structure was obtained.

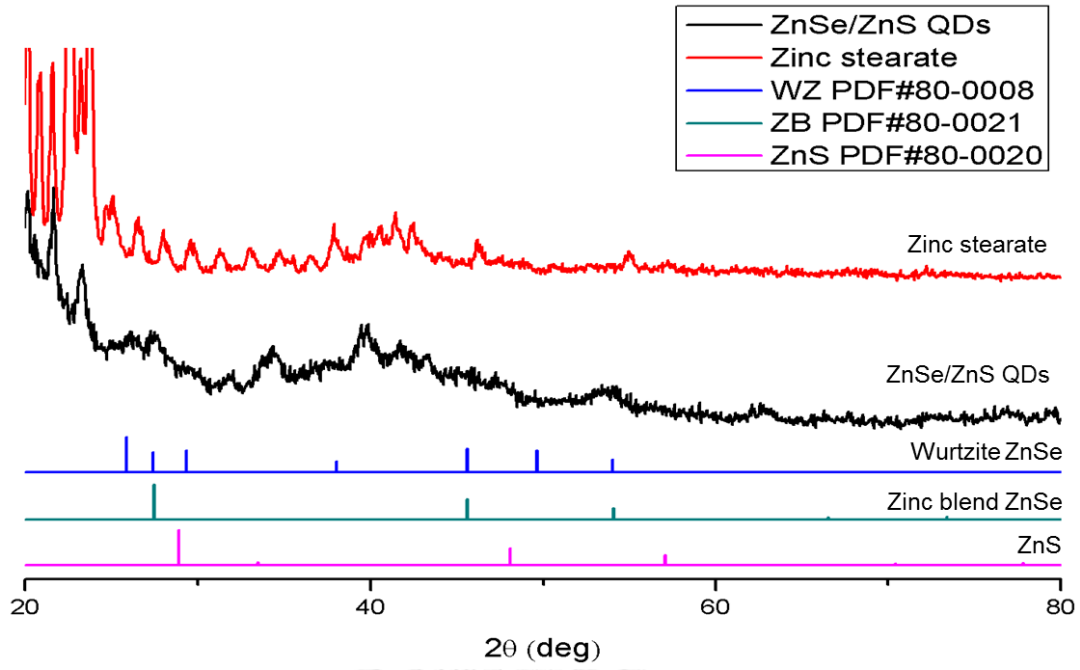

Figure 4.5 XRD patterns of the ZnSe/ZnS QDs in comparison with related standards.

Primarily, TEM was chosen to observe the morphology of synthesized ZnSe and ZnSe/ZnS QDs as core and core/shell respectively. The TEM images in **Figure 4.6 A** and **B** showed the difference in the sizes of core and shell particles. The average diameter of ZnSe core QD was 2.9±0.2 nm, whereas ZnSe/ZnS core/shell QD exhibited larger size of about 3.8±0.4 nm. This result not only confirmed that the particle size of ZnSe/ZnS core/shell nanoparticles grew larger than ZnSe core nanoparticles, but also proved that the shell was coated onto core surface leading to improve efficiency of fluorescence. Moreover, the result in **Figure 4.6 C** and **D** showed the spectra from SEM-EDX elemetal analysis that the signals of zinc, selenide and sulfide were observed.

In **Figure 4.6 C,** the calculated mass % of each metal in ZnSe core QDs are 8.21 for zinc and 6.35 for selenium. For ZnSe/ZnS core/shell QD (**Figure 4.6 D**), the calculated mass % of each metal is 8.56 for zinc, 16.22 for selenium and 0.29 for sulfer. From these results, it can be concluded that ZnSe cores was likely coated with ZnS shell.

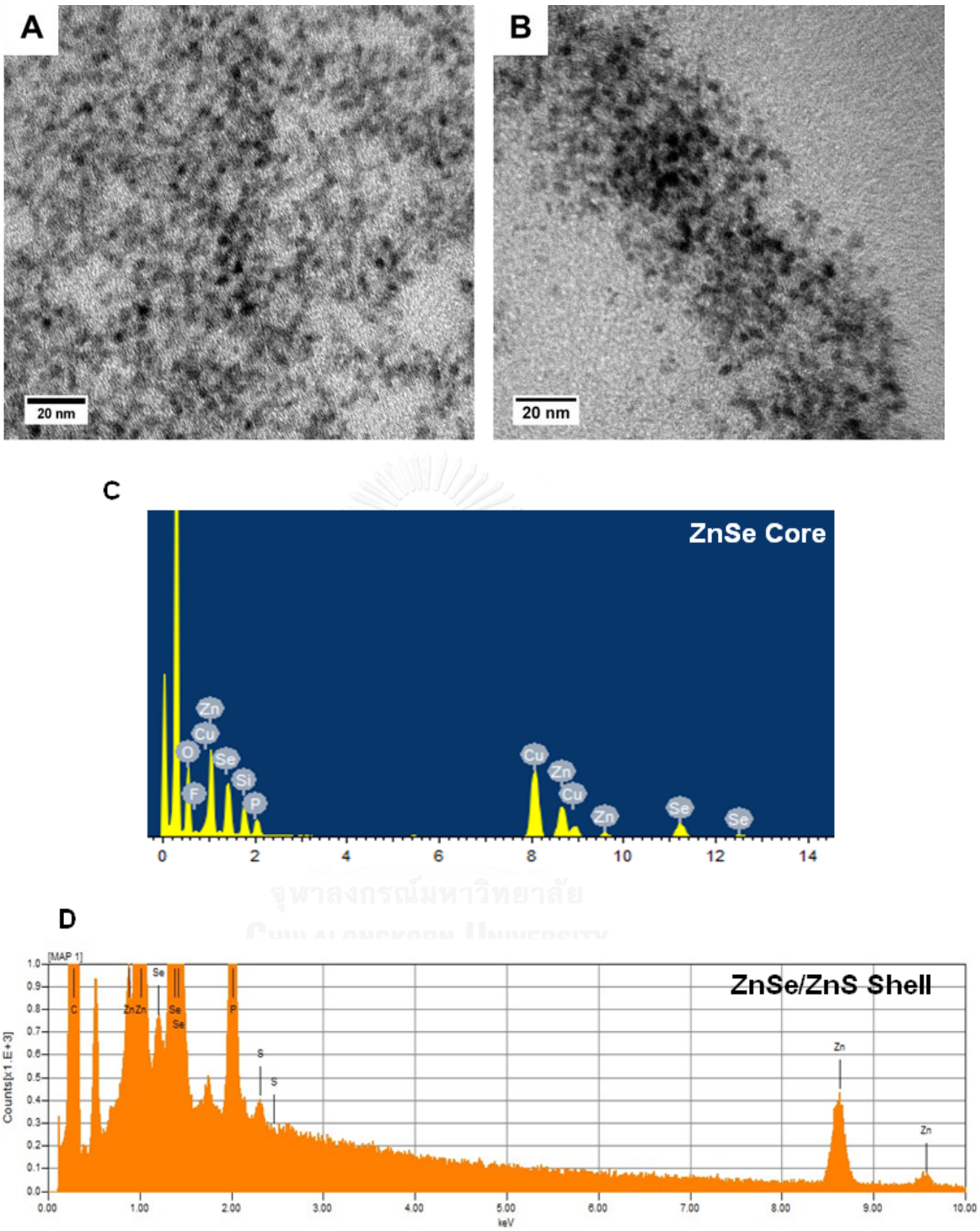

Figure 4.6 TEM images of A) ZnSe core QDs and B) ZnSe/ZnS shell QDs C) SEM-EDX elemental analysis of ZnSe QDs and D) C) SEM-EDX elemental analysis of ZnSe/ZnS QDs

4.2 Synthesis and characterization of QDs conjugated with thiol-PAMAM ligands

4.2.1 QDs with DHLA-PAMAM ligands

4.2.1.1 Synthesis of DHLA conjugated with PAMAM polymer (DHLA-PAMAM ligand)

Firstly, we synthesized thiotic acid (TA) conjugated with PAMAM polymer (TA-PAMAM) and then disulfide bond of TA in TA-PAMAM ligand was reduced to DHLA-PAMAM as mentioned in **Section 3.4.1**. DHLA-PAMAM ligand was easily investigated using Ellman' reagent (DTNB) for checking the presence of thiol group (-SH or R-SH) after ring opening of disulfide bond in thiotic acid. When the thiol group (-SH or R-SH) reacted with Ellman' reagent (DTNB), the TNB^{2-} ion was released in solution. As TNB^{2-} ion has a yellow color, the solution changed from colorless to yellow solution. In **Figure 4.7**, the yellow solution after DHLA-PAMAM ligand reacted with Ellman' reagent was shown.

Figure 4.7 Photograph of Ellman' reagent test of before (left) and after (right) ring opening of the dithiol group in thiotic acid

TA-PAMAM and DHLA-PAMAM ligands were characterized for determining the change in functional groups using Fourier-transform infrared spectroscopy (FT-IR) as shown in **Figure 4.8.** In **Figure 4.8 c)**, thiotic acid (TA) conjugated with PAMAM polymer showed the peaks at wavenumber 1638 and 1562 cm^{-1} corresponding to carbonyl stretching (-C=O) and N-H bending from amide group, respectively, indicating the bond between carboxyl group of TA to one of amine group from PAMAM polymer. The peaks at 3325 and 3226 cm^{-1} corresponded to stretching of primary amine ($-NH_2$) from terminal group in PAMAM polymer.

Furthermore, the carbonyl (-C=O) stretching of carboxyl group from TA in **Figure 4.8a)** was disappeared in products in **Figure 4.8c** and **4.8d.** Therefore, it can be confirmed that TA-PAMAM was successfully synthesis. For DHLA-PAMAM **(Figure 4.8d),** we cannot observed thiol stretching (-S-H) likely resulting from very weak spectra despite the result from Ellman test suggest that thiol group was present.

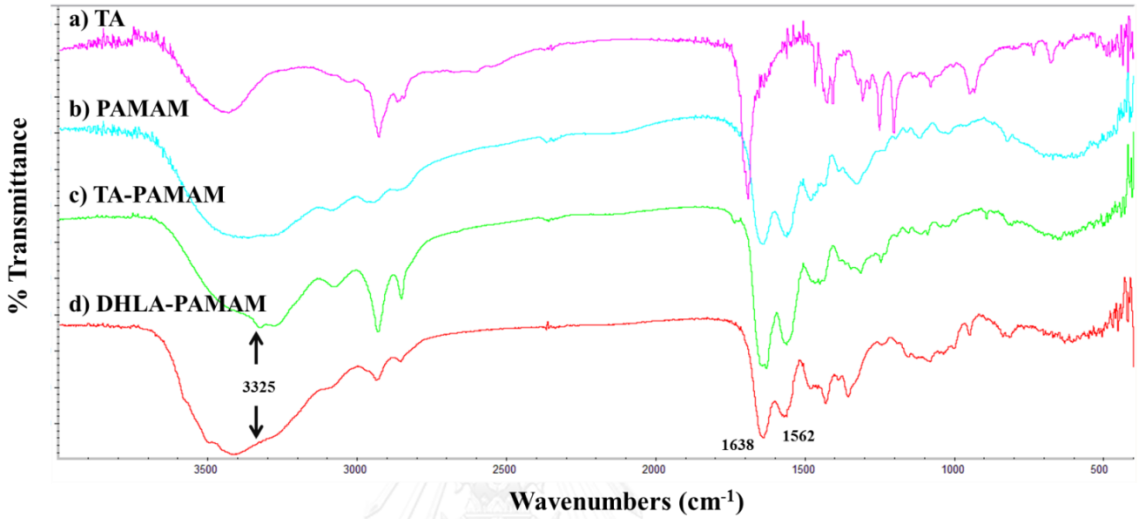

Figure 4.8 IR spectra of reactants and products in DHLA-PAMAM conjugation, a) thiotic acid (TA), b) PAMAM polymer, c) TA-PAMAM and d) DHLA-PAMAM

4.2.1.2 Modification of QDs with DHLA-PAMAM by ligand exchange method (QD-DHLA-PAMAM)

For investigation of conditions for modifying the QDs with DHLA-PAMAM, we used CdSe/ZnS QDs, a more stable and more conventional QDs, to find the suitable condition before applied to ZnSe/ZnS QDs. We modified the CdSe/ZnS QDs using ligand exchange process following a previous report.[55] This ligand exchange method used ethylenediamine (EDA) as an assistant capping ligand to strip off organic ligands on QDs surface because EDA is a small molecule that bind weakly to QD surfaces. When stronger ligands such as dithiol ligands were added, QDs were bound with the new ligands and transferred into the aqueous phase. This method of using an assistant ligand is beneficial as it took short reaction time for completing the ligand exchange.

In this study, we varied the ratios of DHLA-PAMAM ligand:QDs starting from of the thiol:QD ratio of 0.15 M : 2.02×10^{-5} M to the ratio of 3.6 M : 2.02×10^{-5} M. The result found that ligand exchange method using EDA can transfer QD nanoparticles into the aqueous phase completely. At the thiol ligand concentration of lower than 2.4 M, QD-DHLA-PAMAM particles were unstable and aggregated to the phase boundary between the aqueous to organic phases. While upon increasing concentration of thiol ligand, QD-DHLA-PAMAM particles were more dispersibility and less aggregation of particle as shown in **Figure 4.9.**

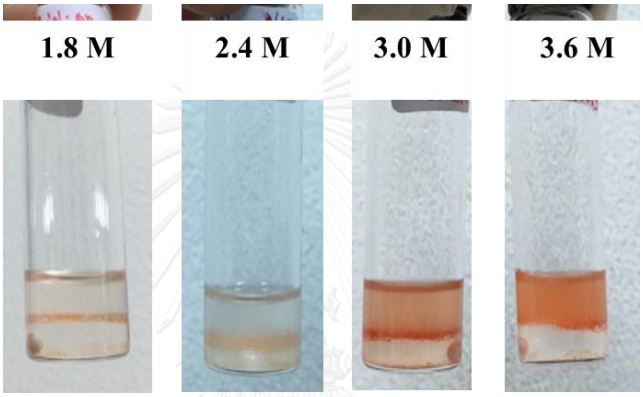

Figure 4.9 Photograph of resulted mixture from ligand exchange process of QD-DHLA-PAMAM using various thiol concentrations at 1.8 M, 2.4 M, 3.0 M and 3.6 M to 2.02×10^{-5} M QDs

4.2.2 QDs with BMPBA-PAMAM ligand

4.2.2.1 Conjugation of QDs with BMPBA-PAMAM by ligand exchange method (QD-BMPBA-PAMAM)

For the limit quantity of BMPBA ligand, we modified BMPBA onto QD surfaces before the BMPBA was conjugated with PAMAM polymer. We used EDA to help removing the original ligand with the same ligand exchange method as in **Section 4.2.1.** For the first step, 0.0036 M BMPBA ligand was used for transferring QDs into the aqueous phase. The result showed that QD nanoparticles can be dispersed and transferred into the aqueous phase completely as shown in **Figure 4.10**

Figure 4.10 Photograph of ligand exchange of QD-BMPBA after finishing reaction

After QDs were modified with BMPBA ligand, the QDs-BMPBA was conjugated with PAMAM polymer by EDC coupling method and purified using a syringe filters. The FT-IR spectra comparing spectra of PAMAM polymer and the resulted ZnSe/ZnS QDs conjugated BMPBA-PAMAM showed that both materials exhibited the peak at wavenumber 3234 cm^{-1} corresponding to secondary amine (N-H stretching). Moreover, the peaks at 1618 and 1635 cm^{-1} corresponding to carbonyl stretching (-C=O) and N-H bending from amide group, respectively. These FTIR spectra suggested the attachment of PAMAM onto QDs as shown in **Figure 4.11.**

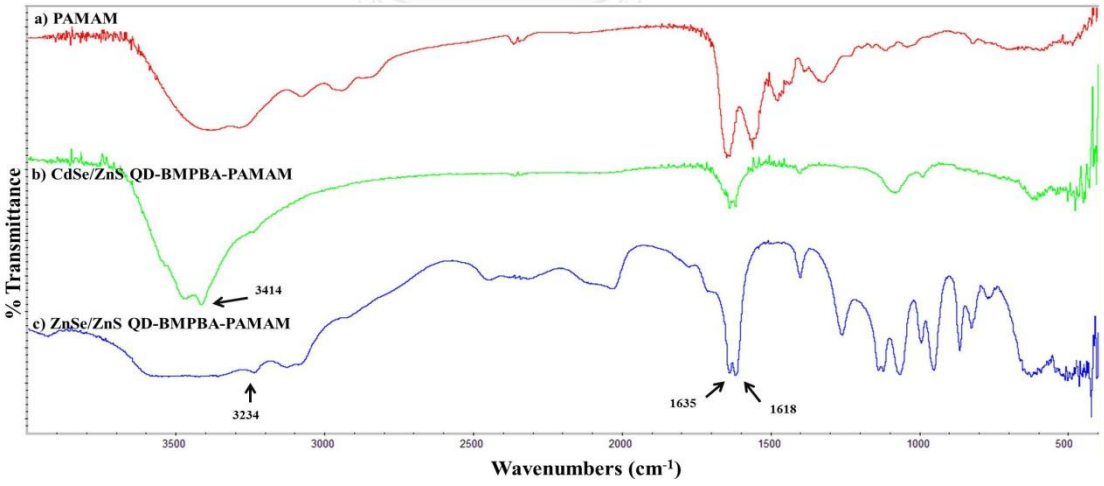

Figure 4.11 Fourier-transform infrared (FT-IR) spectra of PAMAM polymer (a) and QD-BMPBA-PAMAM (b, c)

4.2.3 Comparison of the modified ZnSe/ZnS QD-BMPBA-PAMAM with the modified ZnSe/ZnS QD-DHLA-PAMAM nanoparticles

After obtaining the optimal condition for surface modification of QD nanoparticles based on investigation using CdSe/ZnS nanoparticles, we have applied this process in the surface modification of ZnSe/ZnS nanoparticles. We have used DHLA-PAMAM ligand at the ratio of thiol:QD of 3.6 M : 2.02×10^{-5} M for ZnSe/ZnS QD-DHLA-PAMAM and 0.0036 M : 2.02×10^{-5} M for ZnSe/ZnS QD-BMPBA-PAMAM. The result showed that ligand exchange of ZnSe/ZnS QDs with DHLA-PAMAM ligand yielded a suspension of white, turbid and slowly separation into two phases, while ligand exchange with BMPBA can lead to transferring of ZnSe/ZnS nanoparticles into the aqueous phase completely as in **4.2.2.1** (**Figure 4.12**)

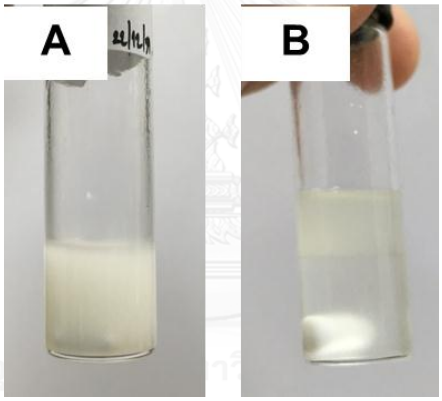

Figure 4.12 Photograph of the mixture from the modification process of ZnSe/ZnS QDs conjugated with two thiol-PAMAM ligands A) ZnSe/ZnS QDs-DHLA-PAMAM and B) ZnSe/ZnS QDs-BMPBA-PAMAM

Figure 4.13A showed the UV absorbance spectra of the modified ZnSe/ZnS QDs-thiol-PAMAM that used two different types of thiol ligands: DHLA (black line) and BMPBA (red line). The results showed that UV absorption spectra of ZnSe/ZnS QDs-BMPBA and ZnSe/ZnS QDs-BMPBA-PAMAM featured first absorption peaks at around 380-400 nm of ZnSe/ZnS QDs, so the modified BMPBA ligand did not affect the absorption property of ZnSe/ZnS QDs, and it can be confirmed the ZnSe/ZnS QDs remained in the solution. On the other hand, the characteristic peaks

of ZnSe/ZnS QDs disappeared in both ZnSe/ZnS QD-DHLA and ZnSe/ZnS QD-DHLA-PAMAM. It indicated aggregation and dissolution of QDs could occur after exposing QDs to the DHLA. Moreover, these results indicated that BMPBA can bind with QDs better than DHLA under the optimal conditions.

For the result of fluorescence spectra, fluorescence of the QDs remained around 400 nm, but some decreases in intensity were observed in both types as shown in **Figure 4.13B.** Therefore, it can be concluded that BMPBA-PAMAM ligand is more effective in binding and transferring ZnSe/ZnS QDs to water than DHLA-PAMAM. Nevertheless, the fluorescence signal of modified ZnSe/ZnS QDs were quenched because sulfur atom in the thiol ligands could disturb on QD surfaces [58, 59]. Not only BMPBA-PAMAM ligand assisted and improved dispersibility of ZnSe/ZnS QD in water solution but its strong binding to QD surface also leads to an increase in stability of particles than DHLA-PAMAM.

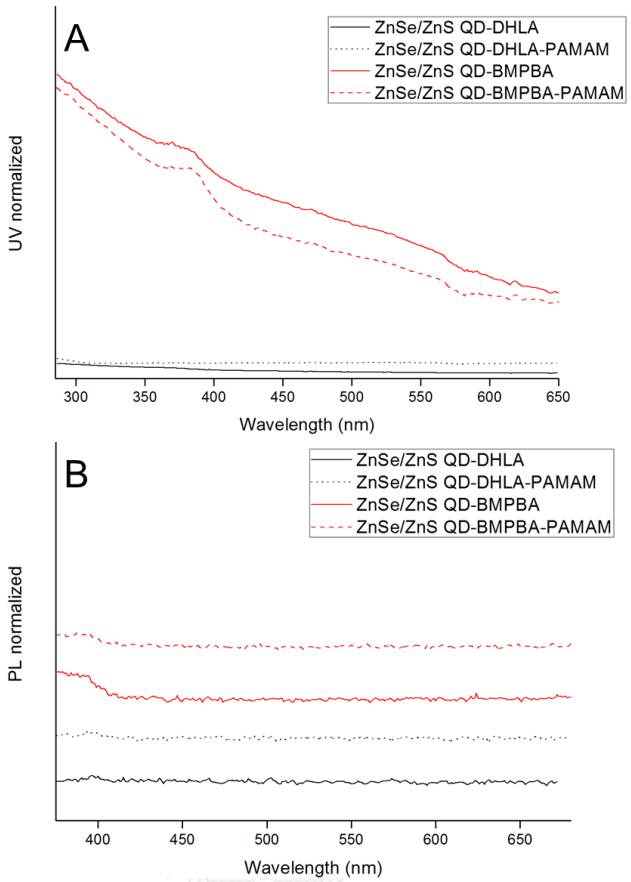

Figure 4.13 UV-visible absorption (a) and fluorescence spectra (b) of ZnSe/ZnS QDs modified with thiol and thiol-PAMAM.

4.4 Cytotoxicity of QDs-BMPBA-PAMAM studied by MTT assay

To evaluate toxicity of modified QDs with thiol-PAMAM, the percent of fibroblast cells (L929) viability was measured by the methylthiazolyldiphenyl-tetrazolium bromide (MTT) assay. In this work, we compared cytotoxicity of two types of quantum dots, cadmium-based QDs (CdSe/ZnS QDs) and zinc-based QDs (ZnSe/ZnS QDs), respectively. QDs were modified with BMPBA and BMPMA-PAMAM at the concentrations of 0, 10 and 100 μg/mL as shown in **Figure 4.14.**

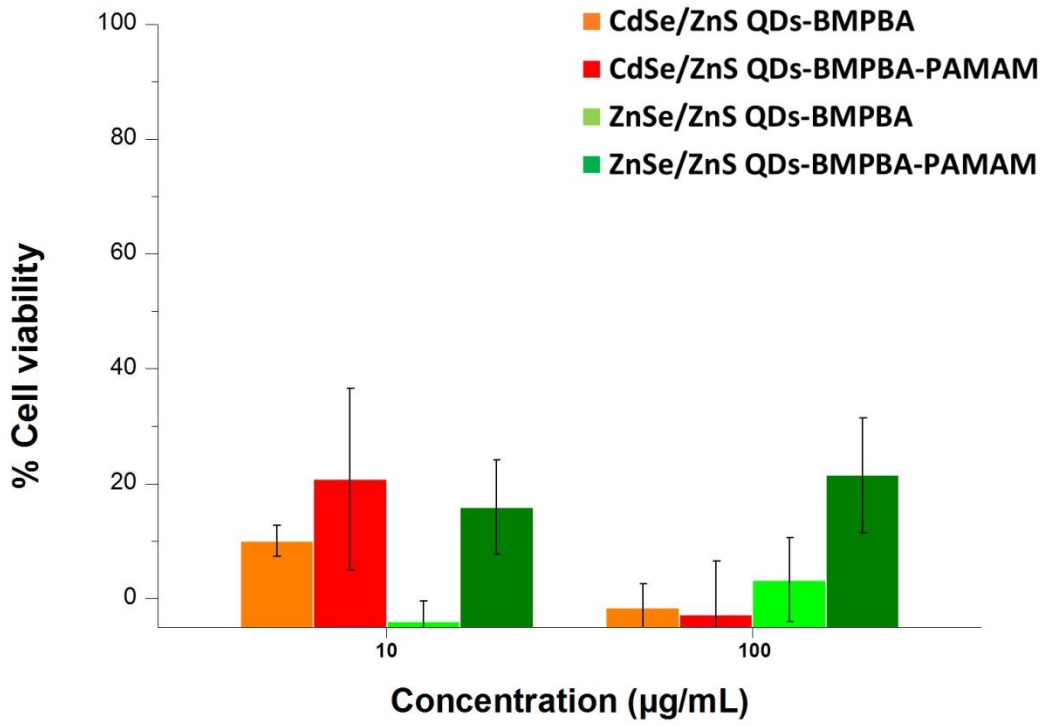

Figure 4.14 Cytotoxicity of Cd-based QDs-BMPBA with PAMAM (red bar), without PAMAM (orange bar), Zn-based QDs-BMPBA with PAMAM (green bar), and without PAMAM (dark green bar) toward L929 mouse fibroblast cell line.

When compared between the modified Cd-based to Zn-based QDs-BMPBA without PAMAM (orange and green bars) at both concentration, the result exhibited that the modified Zn-based QDs-BMPBA without PAMAM induced increasing cell viability significantly (0.026 and 0.002 at 100 and 10 μg/mL respectively, $p<0.05$). It confirms that the use of Zn-based can reduce cytotoxicity to fibroblast cell. In the comparison of PAMAM polymer, the results showed that Cd-based QD-BMPBA with PAMAM (red bar) tended to significantly increase the cell viability at concentration 100 μg/mL (0.036, $p<0.05$). And the result of Zn-based QD-BMPBA-PAMAM also similarly (0.025, $p<0.05$ at concentration of 100 μg/mL, green bar). However, at concentration 10 μg/mL. the result was not shown clearly in both types of QDs-BMPBA with PAMAM and without PAMAM. When, the comparing Cd-based to Zn-based QDs-BMPBA conjugated with PAMAM, the percent cell viability of Zn-based

QDs-BMPBA with and without PAMAM showed higher cell viability than Cd-based QDs at 100 μg/mL significantly (0.009, $p<0.05$).

Although Zn-based QDs-BMPBA-PAMAM at high concentration of 100 μg/mL exhibited higher cell viability than at concentration of 10 μg/mL, it seems to be the effect of precipitated particle influencing disorder cell viability at 10 μg/mL. Hence, it could be implied that that Zn-based QDs have lower toxicity than Cd-based QDs.

For QDs modification with PAMAM polymer, PAMAM affected cell viability for both Cd-based and Zn-based QDs in that the cell viability of QDs with PAMAM was higher than the ones without PAMAM polymer. However, various effects such as aggregation, precipitation of nanoparticles or incomplete ligand modification also influenced the percent of cell viability as the QDs-BMPBA-PAMAM caused lower cell viability compared to thiol-coated QDs previously reported [60].

CHAPTER V

CONCLUSIONS

The ZnSe/ZnS core/shell QDs were successfully synthesized by a hot-injection method in one-pot that could improve the quality and reduce the steps in synthesis of the QDs. The ZnSe/ZnS QDs dispersed into a mixture solution of 1-octadecene as non-coordinate solvent, HDA as surfactant. The average diameters of ZnSe core QD nanoparticles were 2.9±0.2 nm. After coating with ZnS shell, the average diameters of ZnSe/ZnS core/shell QDs were increased to 3.8±0.4 nm. The percent relative fluorescent quantum yield of ZnSe/ZnS core/shell exhibited 50% or about two folds from the ZnSe core. Shell coating was confirmed by TEM and SEM-EDX technique. The effect of time, temperature and ratio of initial precursor were significant factors that affected optical properties of QD nanoparticles. At the optimal condition, ZnSe/ZnS QDs were synthesized using Zn:Se molar ratio of 1:2 with the reaction time of 10 min at 300 °C. For the optical properties, the nanoparticles exhibited the first absorption peak at around 350 nm and emission wavelength at range of 400-450 nm, so they displayed violet-blue emission. The synthesized ZnSe/ZnS QDs have narrow size distribution as observed by the narrow florescent signal with the FWHM of 20-30 nm.

In order to modify the surface of QDs for water dispersibility and biocompatibility, QDs were coated with hydrophilic ligands. To synthesize of thiol ligands conjugated with PAMAM polymer for modification onto QD surfaces, the synthesis of DHLA-PAMAM ligand was achieved as confirmed using FT-IR. The spectra peak showed amine group of PAMAM at the wavenumber of 3325 and 3226 cm^{-1}, carbonyl stretching and N-H bending from amide group at wavenumber 1638 and 1562 cm^{-1}, respectively. For the other thiol ligand, BMPBA ligand, was first coated onto QD surfaces before conjugation with PAMAM. The QDs-BMPBA-PAMAM was characterized using FT-IR to prove the conjugation between QDs, the ligand and the polymer.

Ligand exchange method was successfully developed and utilized for modification of ZnSe/ZnS QDs with thiol-PAMAM for both DHLA-PAMAM and BMPBA-PAMAM ligand leading to transferring and dispersing of ZnSe/ZnS QDs into aqueous phase. The results showed that the BMPBA-PAMAM ligand can bind to QD surfaces more strongly and effectively than DHLA-PAMAM ligand even though BMPBA-PAMAM ligand was used at low concentration. However, the fluorescent signal of modified ZnSe/ZnS QDs were quenched likely because of the disturbance on QD surfaces from sulfur atom in the thiol ligands.

For cytotoxicity studied by methylthiazolyldiphenyltetrazolium bromide (MTT) assay comparing between Cd-based QDs and Zn-based QDs, the results showed that the modified Zn-based QDs become less toxic than the modified Cd-based QDs. Moreover, PAMAM polymer can help increase in the viability of cell comparing with the cells exposing to QDs without PAMAM polymer.

In summary, this work demonstrated the strategies for improving dispersibility and reducing toxicity of fluorescent quantum dot nanoparticles. These concepts can lead to the development of QD nanoparticles in bio-applications in the future.

REFERENCES

[1] Tiwari, J.N., Tiwari, R.N., and Kim, K.S. Zero-dimensional, one-dimensional, two-dimensional and three-dimensional nanostructured materials for advanced electrochemical energy devices. Progress in Materials Science 57(4) (2012): 724-803.

[2] Steiner, D., et al. Zero-Dimensional and Quasi One-Dimensional Effects in Semiconductor Nanorods. Nano Letters 4(6) (2004): 1073-1077.

[3] Liu, J., et al. Fluorescent nanoparticles for chemical and biological sensing. Science China Chemistry 54(8) (2011): 1157-1176.

[4] Jin, S., Hu, Y., Gu, Z., Liu, L., and Wu, H.-C. Application of Quantum Dots in Biological Imaging. Journal of Nanomaterials 2011 (2011): 1-13.

[5] Rosenthal, S.J., Chang, J.C., Kovtun, O., McBride, J.R., and Tomlinson, I.D. Biocompatible quantum dots for biological applications. Chem Biol 18(1) (2011): 10-24.

[6] Geszke-Moritz, M. and Moritz, M. Quantum dots as versatile probes in medical sciences: synthesis, modification and properties. Mater Sci Eng C Mater Biol Appl 33(3) (2013): 1008-21.

[7] Rogach, A.L. Semiconductor Nanocrystal Quantum Dots. Springer Vienna, 2008.

[8] Reiss, P. Synthesis of semiconductor nanocrystals in organic solvents. in Rogach, A.L. (ed.)Semiconductor Nanocrystal Quantum Dots: Synthesis, Assembly, Spectroscopy and Applications, pp. 35-72. Vienna: Springer Vienna, 2008.

[9] Tomczak, N., Jacnzewski, D., Han, M., and Vancso, G.J. Designer polymer–quantum dot architectures. Progress in Polymer Science 34(5) (2009): 393-430.

[10] [Online]. 2013. Available from: http://www.sigmaaldrich.com/materials-science/nanomaterials/quantum-dots.html

[11] [Online]. 2006. Available from: www.aist.go.jp/aist_e/aist_today/2006_21/pict/p22_2.png

[12] Reiss, P. ZnSe based colloidal nanocrystals: synthesis, shape control, core/shell, alloy and doped systems. New Journal of Chemistry 31(11) (2007): 1843.

[13] Sen, T., Haldar, K.K., and Patra, A. Quenching of Confined C480 Dye in the Presence of Metal-Conjugated γ-Cyclodextrin. The Journal of Physical Chemistry C 114(26) (2010): 11409-11413.

[14] Galloway, C.M., Artur, C., Grand, J., and Le Ru, E.C. Photobleaching of Fluorophores on the Surface of Nanoantennas. The Journal of Physical Chemistry C 118(49) (2014): 28820-28830.

[15] Sharma, P., Brown, S., Walter, G., Santra, S., and Moudgil, B. Nanoparticles for bioimaging. Advances in Colloid and Interface Science 123 (2006): 471-485.

[16] Mason, J.N., Tomlinson, I.D., Rosenthal, S.J., and Blakely, R.D. Labeling Cell-Surface Proteins Via Antibody Quantum Dot Streptavidin Conjugates. in Rosenthal, S.J. and Wright, D.W. (eds.),NanoBiotechnology Protocols, pp. 35-50. Totowa, NJ: Humana Press, 2005.

[17] NanoBiotechnologyProtocols. 1 ed. Methods in Molecular Biology. Humana Press, 2005.

[18] Byers, R.J. and Hitchman, E.R. Quantum dots brighten biological imaging. Prog Histochem Cytochem 45(4) (2011): 201-37.

[19] Smith, A.M., Duan, H., Mohs, A.M., and Nie, S. Bioconjugated quantum dots for in vivo molecular and cellular imaging. Adv Drug Deliv Rev 60(11) (2008): 1226-40.

[20] Medintz, I.L., Uyeda, H.T., Goldman, E.R., and Mattoussi, H. Quantum dot bioconjugates for imaging, labelling and sensing. Nat Mater 4(6) (2005): 435-446.

[21] Xiannuo, Z., et al. Cytotoxicity of cadmium-containing quantum dots based on a study using a microfluidic chip. Nanotechnology 23(5) (2012): 055102.

[22] Su, Y., et al. The cytotoxicity of CdTe quantum dots and the relative contributions from released cadmium ions and nanoparticle properties. Biomaterials 31(18) (2010): 4829-4834.

[23] Chen, N., et al. The cytotoxicity of cadmium-based quantum dots. Biomaterials 33(5) (2012): 1238-1244.

[24] Derfus, A.M., Chan, W.C.W., and Bhatia, S.N. Probing the Cytotoxicity of Semiconductor Quantum Dots. Nano Letters 4(1) (2004): 11-18.

[25] Chen, N., et al. The cytotoxicity of cadmium-based quantum dots. Biomaterials 33(5) (2012): 1238-44.

[26] Andrade, J.J., Brasil, A.G., Farias, P.M.A., Fontes, A., and Santos, B.S. Synthesis and characterization of blue emitting ZnSe quantum dots. Microelectronics Journal 40(3) (2009): 641-643.

[27] Ippen, C., et al. ZnSe/ZnS quantum dots as emitting material in blue QD-LEDs with narrow emission peak and wavelength tunability. Organic Electronics 15(1) (2014): 126-131.

[28] Zaman, M.B., Baral, T.N., Zhang, J., Whitfield, D., and Yu, K. Single-Domain Antibody Functionalized CdSe/ZnS Quantum Dots for Cellular Imaging of Cancer Cells. The Journal of Physical Chemistry C 113(2) (2009): 496-499.

[29] Gao, X., Cui, Y., Levenson, R.M., Chung, L.W., and Nie, S. In vivo cancer targeting and imaging with semiconductor quantum dots. Nat Biotechnol 22(8) (2004): 969-76.

[30] Ragusa, A., Zacheo, A., Aloisi, A., and Pellegrino, T. Quantum Dots Designed for Biomedical Applications. in Inorganic Nanoparticles, pp. 257-311: CRC Press, 2010.

[31] Yeh, C.-Y., Lu, Z.W., Froyen, S., and Zunger, A. Zinc-blende–wurtzite polytypism in semiconductors. Physical Review B 46(16) (1992): 10086-10097.

[32] Fang, X., et al. ZnS nanostructures: From synthesis to applications. Progress in Materials Science 56(2) (2011): 175-287.

[33] Tyrakowski, C.M. and Snee, P.T. A primer on the synthesis, water-solubilization, and functionalization of quantum dots, their use as biological sensing agents, and present status. Phys Chem Chem Phys 16(3) (2014): 837-55.

[34] Carion, O., Mahler, B., Pons, T., and Dubertret, B. Synthesis, encapsulation, purification and coupling of single quantum dots in phospholipid micelles for their use in cellular and in vivo imaging. Nat Protoc 2(10) (2007): 2383-90.

[35] Mattoussi, H., Palui, G., and Na, H.B. Luminescent quantum dots as platforms for probing in vitro and in vivo biological processes. Adv Drug Deliv Rev 64(2) (2012): 138-66.

[36] Sperling, R.A. and Parak, W.J. Surface modification, functionalization and bioconjugation of colloidal inorganic nanoparticles. Philos Trans A Math Phys Eng Sci 368(1915) (2010): 1333-83.

[37] [Online]. 2017. Available from: http://lpi.oregonstate.edu/mic/dietary-factors/lipoic-acid

[38] Lee, H.J., et al. Robust carboxylic acid-terminated organic thin films and nanoparticle protectants generated from bidentate alkanethiols. Langmuir 29(33) (2013): 10432-9.

[39] Srisombat, L.O., Park, J.S., Zhang, S., and Lee, T.R. Preparation, characterization, and chemical stability of gold nanoparticles coated with mono-, bis-, and tris-chelating alkanethiols. Langmuir 24(15) (2008): 7750-4.

[40] Labieniec-Watala, M. and Watala, C. PAMAM dendrimers: destined for success or doomed to fail? Plain and modified PAMAM dendrimers in the context of biomedical applications. J Pharm Sci 104(1) (2015): 2-14.

[41] Taghavi Pourianazar, N., Mutlu, P., and Gunduz, U. Bioapplications of poly(amidoamine) (PAMAM) dendrimers in nanomedicine. Journal of Nanoparticle Research 16(4) (2014).

[42] Rajasekhar, D. and Liao, P.-C. Patents and the Development on Polymer based Nanomaterial (PAMAM Dendrimer) for Biomedical Applications. in Recent Patents on Biomedical Engineering, pp. 159-174: Bentham Science Publishers, 2012.

[43] Tomalia, D.A., et al. A New Class of Polymers: Starburst-Dendritic Macromolecules. Polym J 17(1) (1985): 117-132.

[44] Esfand, R. and Tomalia, D.A. Poly(amidoamine) (PAMAM) dendrimers: from biomimicry to drug delivery and biomedical applications. Drug Discovery Today 6(8) (2001): 427-436.

[45] Dendritech, I. PAMAM polymer [Online]. 2017. Available from: http://www.dendritech.com/pamam.html

[46] Svenson, S. and Tomalia, D.A. Dendrimers in biomedical applications—reflections on the field. Advanced drug delivery reviews 64 (2012): 102-115.

[47] Reiss, P., Quemard, G., Carayon, S., Bleuse, J., Chandezon, F., and Pron, A. Luminescent ZnSe nanocrystals of high color purity. Materials Chemistry and Physics 84(1) (2004): 10-13.

[48] Wang, A., et al. Bright, efficient, and color-stable violet ZnSe-based quantum dot light-emitting diodes. Nanoscale 7(7) (2015): 2951-9.

[49] Susumu, K., Uyeda, H.T., Medintz, I.L., Pons, T., Delehanty, J.B., and Mattoussi, H. Enhancing the Stability and Biological Functionalities of Quantum Dots via Compact Multifunctional Ligands. Journal of the American Chemical Society 129(45) (2007): 13987-13996.

[50] Liu, W., Choi, H.S., Zimmer, J.P., Tanaka, E., Frangioni, J.V., and Bawendi, M. Compact Cysteine-Coated CdSe(ZnCdS) Quantum Dots for in Vivo Applications. Journal of the American Chemical Society 129(47) (2007): 14530-14531.

[51] Zhao, Y., et al. Synthesis and grafting of folate-PEG-PAMAM conjugates onto quantum dots for selective targeting of folate-receptor-positive tumor cells. J Colloid Interface Sci 350(1) (2010): 44-50.

[52] Higuchi, Y., et al. Polyamidoamine dendrimer-conjugated quantum dots for efficient labeling of primary cultured mesenchymal stem cells. Biomaterials 32(28) (2011): 6676-82.

[53] Figueroa, E.R., Lin, A.Y., Yan, J., Luo, L., Foster, A.E., and Drezek, R.A. Optimization of PAMAM-gold nanoparticle conjugation for gene therapy. Biomaterials 35(5) (2014): 1725-34.

[54] Das, A., Sanjayan, G.J., Kecskés, M., Yoo, L., Gao, Z.-G., and Jacobson, K.A. Nucleoside conjugates of quantum dots for characterization of G protein-

coupled receptors: strategies for immobilizing A 2A adenosine receptor agonists. Journal of nanobiotechnology 8(1) (2010): 11.

[55] Dai, M.-Q. and Yung, L.-Y.L. Ethylenediamine-Assisted Ligand Exchange and Phase Transfer of Oleophilic Quantum Dots: Stripping of Original Ligands and Preservation of Photoluminescence. Chemistry of Materials 25(11) (2013): 2193-2201.

[56] Dabbousi, B.O., et al. (CdSe)ZnS Core–Shell Quantum Dots: Synthesis and Characterization of a Size Series of Highly Luminescent Nanocrystallites. The Journal of Physical Chemistry B 101(46) (1997): 9463-9475.

[57] Yu, W.W., Wang, Y.A., and Peng, X. Formation and Stability of Size-, Shape-, and Structure-Controlled CdTe Nanocrystals: Ligand Effects on Monomers and Nanocrystals. Chemistry of Materials 15(22) (2003): 4300-4308.

[58] Kalyuzhny, G. and Murray, R.W. Ligand effects on optical properties of CdSe nanocrystals. The Journal of Physical Chemistry B 109(15) (2005): 7012-7021.

[59] Wuister, S.F., de Mello Donega, C., and Meijerink, A. Influence of thiol capping on the exciton luminescence and decay kinetics of CdTe and CdSe quantum dots. The Journal of Physical Chemistry B 108(45) (2004): 17393-17397.

[60] Casas, J.S., et al. Synthesis, characterization and in vitro toxicity assessment of DMPS-capped CdTe quantum dots. Polyhedron 70 (2014): 77-84.

APPENDIX

Figure A1 The photograph of ZnSe/ZnS QDs under a black light lamp

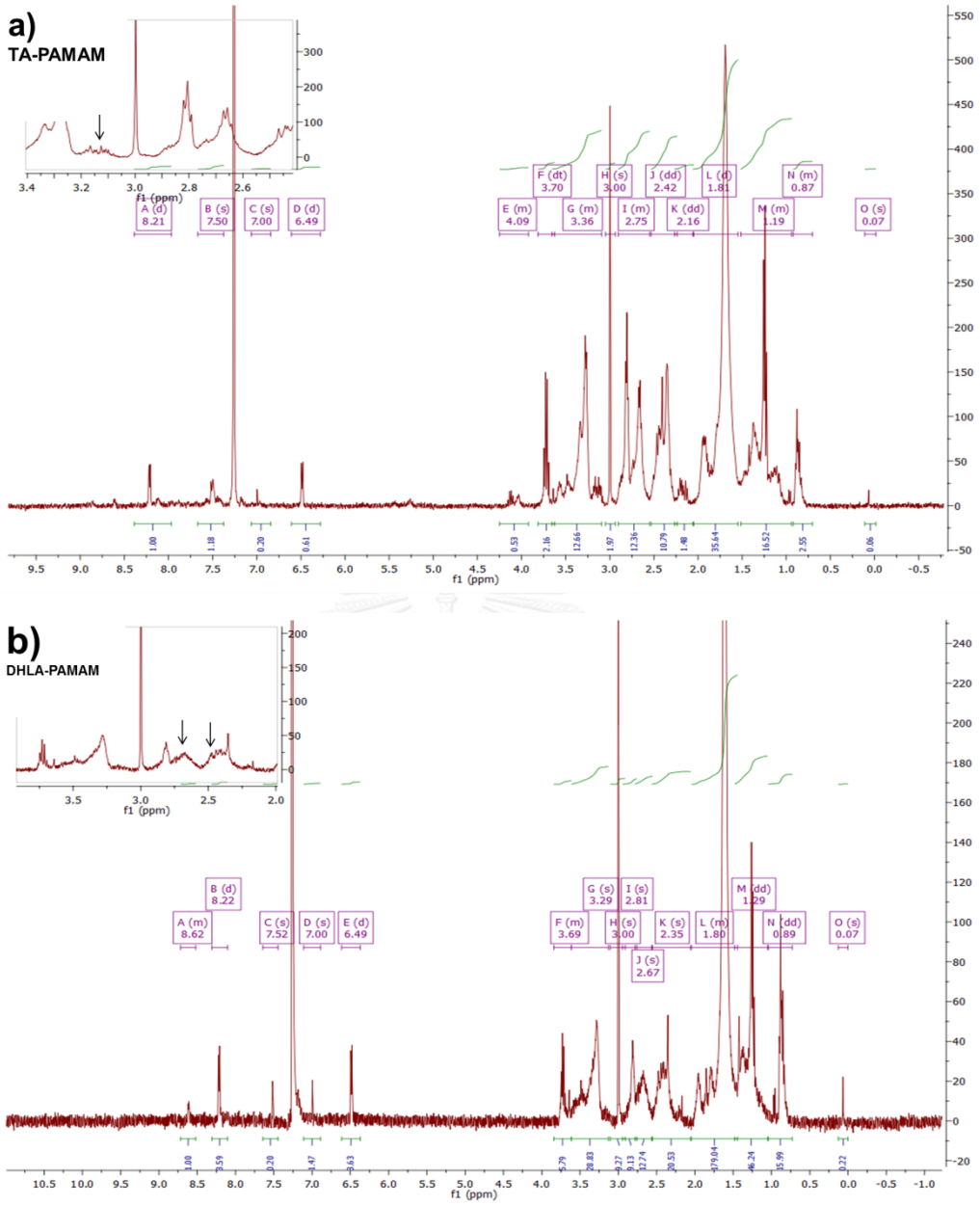

Figure A2 The ^{1}H-NMR spectra of a) TA-PAMAM (before ring opening) compare with b) DHLA-PAMAM (after ring opening)

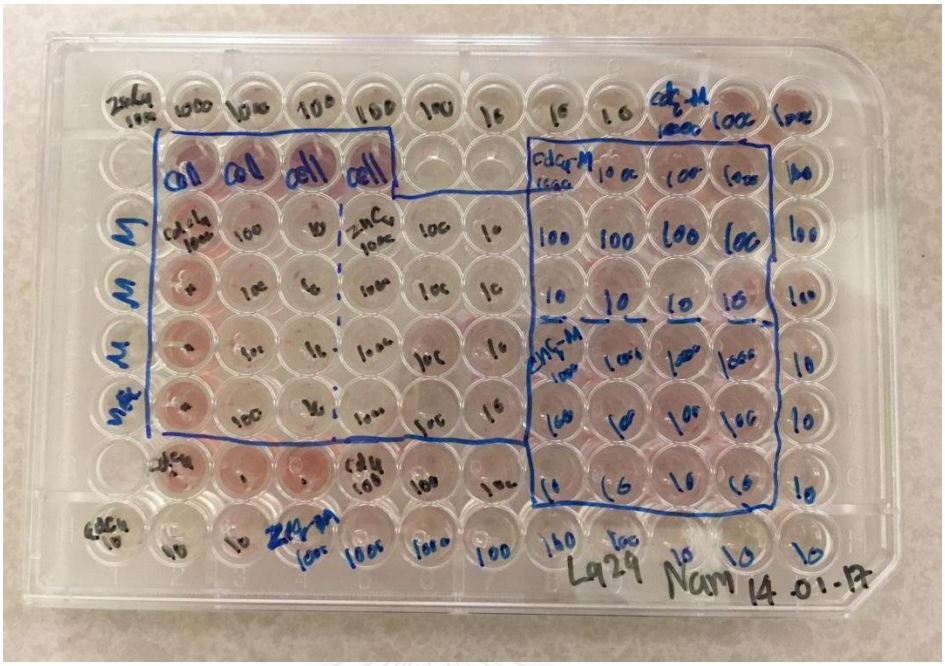

Figure A3 The photograph of cytotoxicity studied comparing modified Cd-based QDs and modified Zn-based QDs using MTT assay

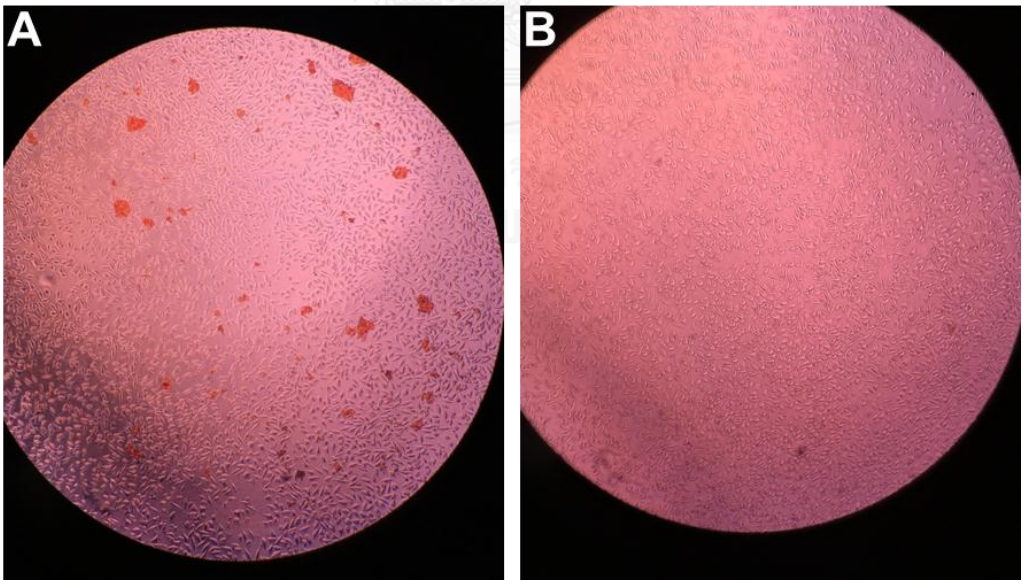

Figure A4 The photographs of cell viability with A) CdSe/ZnS QDs-BMPBA-PAMAM and B) ZnSe/ZnS QDs-BMPBA-PAMAM

VITA

Miss Radawan Palikanon was born on January 9, 1991 in Bangkok, Thailand. She graduated with Bachelor's Degree in Chemistry from Faculty of Science, Chulalongkorn University in 2013. She continued her Master's Degree of Science in Petrochemistry and Polymer Science, Faculty of Science, Chulalongkorn University. She became a member of Materials Chemistry and Catalysis Research Unit under the supervision of Dr. Numpon Insin. On 2-3 February 2017, she attended The 17th Pure and Applied Chemistry International Conference 2017 in the title of "Preparation of water-dispersible ZnSe/ZnS core-shell quantum dots and investigation of their cytotoxicity" by poster presentation.

Her present address is 56/180 Soi Ramintra34 Yaek 21, Ramintra Road, Tarang, Bangkhen, Bangkok 10230

Email address: praew_radawan@hotmail.com